Equilibrium partitioning of naphthenic acid mixture part 2: Crude oil extracted naphthenic acids.

Are Bertheussen*, Sébastien Simon and Johan Sjöblom

Ugelstad Laboratory, Department of Chemical Engineering, the Norwegian University of Science and Technology (NTNU), N-7491 Trondheim, Norway

Highlights

- Composition of naphthenic acids by GC/MS
- Partitioning of acids to determine water quality of produced water
- Equilibrium partitioning of crude oil extracted naphthenic acids vs pH

Abstract:

Crude oil naphthenic acids can partition into the water phase during oil production. Variations in production parameters such as temperature, pressure, pH and water cut affect partitioning. In a previous article, a method has been developed to determine the partition ratio for mixtures of naphthenic acids and tested on a commercial acid mixture. In this study, the method is implemented on a naphthenic acid mixture extracted from an acidic crude oil. Compositional analysis of the extracted acid mixture reveals a broad structural distribution consisting mainly of saturated ring structures with 2 to 3 rings. Examination of the GC/MS method revealed a distribution bias towards low molecular weight compounds and a correction method was explained and applied. The equilibrium partitioning as a function of pH for the acid mixture and molecular mass ranges within the acid mixture was determined by GC/MS. An extracted crude oil acid mixture dissolved in toluene was used as oil phase and 3.5wt.% NaCl aqueous buffers were used as water phase. Dividing the acid mixture into molecular weight ranges, characterized by a single partition ratio P_{wo} allowed the oil-water partitioning to be successfully modelled. The variation of the cologarithm of the partition ratio pP_{wo} with naphthenic acid molecular weight was compared with previously published experimental and simulated data. The presence of calcium reduced the partitioning of the acid mixture at high pH for larger acid molecules. Analysis of the resulting oil phase revealed a calcium content consistent with oil-soluble calcium naphthenate, in agreement with results found for a commercial acid mixture.

*To whom correspondence should be addressed.

Telephone: (+43) 73 55 09 24.
E-mail: are.bertheussen@ntnu.no

Keywords
Equilibrium partitioning
GC/MS
Naphthenic acids
Partition ratio

1. Introduction

Production of acidic crude oil is increasing both worldwide and in the North Sea [1]. With expected growth in deep-sea and arctic production [2], new subsea separator designs are in development to match the new requirements [3, 4]. It is therefore needed to have better tools to model the oil water separation as well as the quality of the separated phases. Variations in pressure and temperature during production can induce the partitioning of crude oil components such as naphthenic acids into the produced water. The presence of these components can alter the stability of water droplets in oil as recently shown [5, 6] and oil droplets in water [7]. This paper is the second in a series of two which will discuss and explore the composition and equilibrium partitioning of naphthenic acid mixtures.

2. Theory

2.1. Definition and prevalence

Naphthenic acids are part of the resin group in crude oils. They are generally described by the raw formula $C_nH_{2n+Z}O_2$ [8] with a molecular weight of around 200-700 g/mol [9]. As with other crude oil groups, naphthenic acid structures are complex. The analysis of some crude oil acids reveal that more than half of the identified acidic structures contained additional functional groups of oxygen, nitrogen, aromatics or sulphur like alkyl sulphonic acid [10-12]. A new term, naphthenic acid fraction components (NAFC), was defined by Headley, et al. [13], allows the encompassment of a large

number of structures with functional groups containing hetero elements oxygen, sulphur, nitrogen, aromatic rings and unsaturations in crude oil.

Naphthenic acids have been linked to downstream corrosion [14], emulsion formation [15, 16], deposition on processing units [17] and formation pore blockage [18]. Multiple authors have applied mass spectroscopy to characterize naphthenic acids [5, 10-12, 19-27]. Mass spectroscopy have some limitations that need to be accounted for. For instance, Clingenpeel, et al. [28] and Rowland, et al. [29] analyzed surface active compounds including naphthenic acids in bitumen and deasphalted bitumen with FT-ICR MS. They stressed the importance of prior fractionation of the sample by demonstrating that easily ionizable low molecular weight compounds hide the presence of less ionizable and larger compounds. Clingenpeel, et al. [28] also demonstrated that it was these larger and previously hidden surface active compounds which contributed most to the emulsion stability. Ligiero [5] studied the water-soluble compounds in resolved waters from several crude oils with ESI-MS and surprisingly found the crude oil with the lowest TAN value (0.1) to give the broadest naphthenic acid distribution in the resolved water, some of which had asphaltene-like characteristics (double bond equivalent (DBE) > $0.46C_n$). However, the comparison involves only three crude oils, and therefore needs to be extended. When exact molecular structure is not essential, simpler naphthenic acid analysis methods have been developed for standard GC/MS instrumentation. Derivatization with N-methyl-N-(t-butyldimethylsilyl) trifluoroacetamide (MTBSTFA) produces stable ion fragment [M+57] where M is the molecular weight of the naphthenic acid [19]. This method allows for crude classification based on carbon number and hydrogen deficiency *Z* of naphthenic acids peaks within the unresolved GC/MS elution hump [21].

The partitioning of naphthenic acids to the water phase have been studied by several authors [23, 30, 31]. Stanford, et al. [23] extracted crude oil acids with pH neutral water and detected water soluble acids up to C_{41}(~600 g/mol) with FT-ICR MS. Havre, et al. [30] found that the partition ratio varied depending on the molecular weight of the acids and that naphthenic acids in crude oil water systems had a pK_a around 4.9. Celsie, et al. [32] simulated the effect of temperature on naphthenic acid partitioning and found that the partition ratio goes towards unity upon increasing temperature. This qualitatively correlates with the finding of Bostick, et al. [33], studying the concentration of different water soluble organics as a function of pH, salinity, pressure and temperature, who found that increased temperature did not affect the total amount of polar organics in the water phase, but

increased the concentration of C_{10}-C_{20} components while decreasing the concentration of C_6-C_{10} components. Other factors like the presence of calcium has been shown to affect naphthenic acids behavior in oil water systems [9, 34-38]. In the presence of calcium, oil-soluble calcium naphthenate can form [39] which can cause problems in downstream processing [40]. In order to combat the naphthenate problems [17], Dyer, et al. [41] made a huge matrix of experimental results on the topic by screening dozens of carboxylic acids in systems with various pH values, concentrations and water phase compositions, before it was discovered that a specific family of naphthenic acids named ARN was the main component behind the calcium naphthenate problems [42].

This article will study the equilibrium partitioning of an extracted crude oil acid mixture, determine acid partition ratios and present insight into at which pH the phase change occurs.

2.2. Modelling of partition ratio with pH

A thermodynamic model for the partitioning of naphthenic acids applied in previous work by Bertheussen, et al. [43 44] is presented. All concentrations are in mol/L, unless otherwise stated.

In an oil-water system, protonated acids would partition themselves between the oil and water phase described by the following partition constant

$$K_{wo,HA} = \frac{[HA]_w}{[HA]_o} \qquad (1)$$

where $[HA]_w$ represents the protonated acid concentration in the water phase, $[HA]_o$ represents the acid concentration in the oil phase and $K_{wo,HA}$ represents the partition constant of the acid. As described in previous work [43] it was favored to use the partition ratio, P_{wo}, instead to avoid considering dimers in the oil phase [45]. Although the partition ratio is not a constant because of its dependence on concentration, it is a practical term with regards to measurements. The partition ratio of 4-heptylbenzoic acid was shown to remain almost constant with concentration [46]. The partition ratio accounts for the non-ionized compounds in each phase as seen in Equation 2.

$$P_{wo} = \frac{[HA]_w}{[HA]_{o,tot}} = \frac{[HA]_w}{[HA]_o + 2[(HA)_2]_o} \qquad (2)$$

Water phase dissociation of acids are described by the following dissociation constant

$$K_{a,HA} = \frac{[A^-]_w[H^+]}{[HA]_w} \quad (3)$$

where $[A^-]_w$ represents the concentration of dissociated acid in the water phase and $K_{a,HA}$ represents the dissociation constant of the acid.

The following mass balance is valid for a system without precipitation.

$$[HA]_{o,init}\, V_o = [HA]_{w,tot} V_w + [HA]_{o,tot} V_o \quad (4)$$

where $[HA]_{o,init}$ represents the initial concentration of acid in the oil phase, and $[HA]_{w,tot}$ represents the sum of dissociated and undissociated acids in the water phase. The terms V_o and V_w denote the volume of the oil and water phase.

Combining equations 2, 3, and 4 gives expressions for the total acid concentration in the oil and water phase.

$$[HA]_{w,tot} = \frac{[HA]_{o,init}}{\frac{[H^+]}{P_{wo,acid}(K_{a,HA}+[H^+])}+\frac{V_w}{V_o}} \quad (5)$$

$$[HA]_{o,tot} = \frac{[HA]_{o,init}}{1+\frac{V_w P_{wo,acid}(K_{a,HA}+[H^+])}{V_o[H^+]}} \quad (6)$$

It is assumed that the deprotonated acid [A^-] is completely insoluble in oil phase. The formation of aggregates was not taken into account in the model presented in Equations 5 and 6.

This study is expanding on and comparing with previous work performed on a commercial acid mixture. In this study, two crude oil acid mixtures will be characterized, mainly by GC/MS. Then the equilibrium partitioning of an extracted crude oil acid mixture will be considered over the pH range. The partition ratio P_{wo} will be obtained through fitting Equations 5 and 6 with a constant pK_a of 5. The use of this pK_a value will be justified in section 4.2. The effect of calcium on the partitioning will be also be evaluated. Then the P_{wo} obtained in this work will be compared with values from the literature, and with measurements using a model naphthenic acid, 4-heptylbenzoic acid.

3. Materials and methods

3.1. Chemicals

The chemicals used to perform the partitioning experiments and GC/MS analysis have already been presented in a part I article of this series. Additional chemicals were used in this new study. They were used as received and not further purified. Boron trifluoride-methanol (Sigma Aldrich, 14wt.%), 4-heptyl benzoic acid (VWR, 99%), tridecanoic acid (Fluka, 99.7%), heptane (Sigma Aldrich, >99%) and ultra-pure water (MilliQ resistivity of 18.2 MΩ·cm millipore). The extracted crude oil acid mixtures, A and B, were provided by Equinor. The acids were obtained through the Acid-IER method [47] performed at Equinor Research Centre Rotvoll and were delivered as amber colored 1.5wt.% solutions in 1:1(wt.) toluene and isopropanol. The crude oils used for extraction come from the same North Sea reservoir, but from different wells. More data are listed in Table 1. The crude oil acid solutions were evaporated to a stable weight at 60°C under nitrogen convection to prepare toluene stock solutions. The color of the dried acids was dark brown.

Table 1 Characteristics of the extracted crude oil acids and their parent crude oil. Data kindly provided by Equinor.

	Extracted crude oil acid mixture A	Extracted crude oil acid mixture B
Average molecular weight**	438 g/mol	454 g/mol
Extraction yield	90%	94%
TAN of the parent crude oil [mg_{KOH}/g]	1.7	3.1
Water-cut well at sampling time	58%	19%

**Average values calculated from titration of the isolated acids by assuming monoprotic acids as explained in Mediaas, et al. [47]

3.2. Characterization

A Bruker Avance nuclear magnetic resonance (NMR) spectrometer (400 MHz) was used to obtain hydrogen 1 (^1H) NMR spectra on a 1% solution in $CDCl_3$. The number of scans used was 8. The Laboratory SGS Multilab (Evry, France) determined the elemental composition by thermal conductivity measurements for C, H, and N, by infrared measurements for O and S, by mineralization and ICP/AES for Ca and Na and potentiometric titration for Cl.

3.3. Equilibrium partitioning

The partitioning of naphthenic acids were determined according to a procedure developed in Bertheussen, et al. [44]. The procedure is briefly recalled below. At least 2 parallels were performed per condition tested.

3.3.1. In presence of monovalent cations

4 mL of 3.3 mM (1.4 g/L) for pH lower than 10, 1.65 mM (0.7 g/L) for pH higher than 10, extracted crude oil acid mixture A in toluene were mixed with 4 mL of aqueous solution containing 3.5wt.% NaCl and a buffer (Table 2) for 1 day at 250 rpm. Aliquots of oil and aqueous phase were recovered after centrifugation (11000 rpm, 30 minutes). The pH of the aqueous phase was then measured, and 3 mL was adjusted to pH < 2. Then the, now protonated, naphthenic acids were back-extracted in toluene (3 mL, 24 h shaking). Note that, after centrifugation, the centrifugation tube used for the samples prepared at pH 11 and pH 12 had a light brown colored layer along the tube wall in the water phase.

3.3.2. In the presence of divalent cation, Ca^{2+}.

The procedure was like the method described in part 3.3.1 with the following modification.

- In addition to NaCl 3.5wt.% and buffers, the aqueous phase also contained 10 mM $CaCl_2$.
- pH 11 samples were not buffered owing to the incompatibility between $NaHCO_3$ and $CaCl_2$. This solution did not contain buffer and the initial pH was 11.5 to obtain the correct equilibrium pH.
- Tests were performed by washing the equilibrated oil phase with low pH buffer to determine the influence of calcium naphthenate on the derivatization reaction, but results were similar as without washing.
- Finally, it was not observed any brown layer on the centrifugation tube wall when the water phase contained $CaCl_2$.

Elemental analysis of the resulting oil phase after high pH partitioning was performed. High volumes (350 mL of both phases) were required to obtain enough dry sample. Only extracted crude oil acid B was used in this experiment due to the limited amount of extracted crude oil acids available (0.6 g of acid mixture A and 0.5 g of acid mixture B). Due to the similar origin and statistically insignificant mass distribution difference between acid mixtures A and B (see section 4.1.2.2, Figure 6 and Figure 7), elemental analysis results obtained with extracted crude oil acid B were assumed representable to explain partitioning results obtained with extracted crude oil acid A. Likewise, due to the limited amount of sample, only one elemental analysis determination was performed.

3.3.3. Model acid 4-heptylbenzoic acid

The equilibrium partitioning for the model acid 4-heptylbenzoic acid was performed similarly as in section 3.3.1, except the concentration of this acid was 1 mM in toluene and 10 mL of each phase were put into contact. Equal volumes of internal standard (tridecanoic acid 0.5 mM in toluene) was added to samples prior to solvent evaporation under nitrogen at 50 degrees. Dry samples were derivatized by addition of 1.5 mL 14wt.% Boron trifluoride-methanol solution before stirring in a 60°C waterbath for 1 h. 2 mL heptane and 1.5 mL MQ water was added to the sample vials before shaking for 30 min at 250 rpm. The final heptane phase was analyzed with GC/FID at Equinor Research Centre Rotvoll and quantitative results obtained by comparison with calibration curves.

Table 2 List of different aqueous buffers prepared [48]. 3.5wt.% NaCl was also present in these buffers.

pH	Buffers
4	0.1 M CH_3COOH adjusted with NaOH
6-7.9	0.1 M KH_2PO_4 adjusted with NaOH
8.4-9	0.025 M Borax adjusted with HCl
9.5-10	0.025 M Borax adjusted with NaOH
11	0.05 M $NaHCO_3$ adjusted with NaOH
12	0.01 M NaOH

3.4. GC/MS analysis of the extracted naphthenic acids.

The GC/MS analysis was developed in Bertheussen, et al. [44]. The procedure is briefly summarized.

3.4.1. Derivatization and analysis

270 mg of a 0.23 mM capric acid in toluene solution (used as internal standard), was added to 1.6 g of the sample to be analyzed. 0.36 g of this solution was mixed with 0.04 g of N-tert-Butyldimethylsilyl-N-methyltrifluoroacetamide with 1% tert-Butyldimethylchlorosilane (MTBSTFA + 1% TBDMSCl) and heated at 65°C for 30 minutes. Then the derivatized sample was analyzed (injection volume 1.5 μL) on an Agilent GC(7890)/MS(5977). The separation was performed on an Agilent J&W DB-1HT Non-polar, 100% Dimethylpolysiloxane, capillary column (30m×0.25mm×0.10 μm film thickness) in splitless mode and at a flow rate of 1 mL helium per minute. The inlet temperature was 360°C and the GC temperature program was the following. The temperature was initially 100°C for 5 minutes, then increased to 350°C at a rate of 5°C/min. This maximum temperature was finally held for 10 minutes.

3.4.2. Identification of naphthenic acid composition by GC/MS

Analysis were performed using the Masshunter Acquisition Data software. First mass spectra were extracted from the chromatogram peak, with a height filter, relative height > 0.1% of largest peak. Spectra from corresponding injection of blank solvents were subtracted from the sample data. The n, Z distribution of naphthenic acids was determined from m/z values using the following procedure: First if m/z is comprised between (x-1).7 (included) and (x).7, then it is rounded to x. For instance:

- m/z values of 237.4 or 237.6 would be rounded to 237.
- m/z values of 237.7 or 238.69 would be rounded to 238.

The integer m/z values then allow for the determination of n and Z using the table presented in the supplementary information (Table S1).

3.4.3. Quantification by GC/MS

Different chromatograms could be obtained from raw data:

- Total ion chromatograms (TIC) represent the sum of all intensities for all m/z values included in the mass scan.
- Extracted ion chromatograms (EIC) represent the sum of intensities for a specific mass or mass range.

EIC were obtained from TIC and used, after subtraction of solvent blanks and integration, to obtain naphthenic acid concentration after normalization with the peak of the capric acid (internal standard) and comparison with a calibration curve built beforehand. The calibration curves were performed as advised by the manufacturer. This determination is further explained in section 4.2.

4. Results and Discussion

4.1. Characterization

4.1.1. Characterization by elemental analysis and NMR

The average molecular weight of NA mixtures A and B was reported by Equinor as 438 g/mol and 454 g/mol respectively (Table 1) by determining the TAN and the mass of the extracted acids. The average molecular weight of the extracted acids can be determined by TAN titration by combining the two equations 7 and 8 [47]

$$n_{acid} = \frac{(V_{EP} - V_b) \cdot C_{titrant}}{1000} \qquad (7) \qquad\qquad TAN = \frac{(V_{EP} - V_b) \cdot C_{titrant} \cdot M_{KOH}}{m_{sample}} \qquad (8)$$

into Equation 9

$$M_{acid} = \frac{m_{sample} \cdot 1000}{(V_{EP} - V_b) \cdot C_{titrant}} = \frac{M_{KOH} \cdot 1000}{TAN} \qquad (9)$$

where n_{acid}, M_{acid} and m_{sample} is the number of mole, average molecular weight and mass of the extracted acid mixture respectively in the units moles, g/mol and g. M_{KOH} is the molecular mass of potassium hydroxide in g/mol. V_{EP} and V_b are the volume of titrant required to the equivalence point for sample and pure solvent (blank) respectively, in mL. $C_{titrant}$ is the concentration of the titrant used, in mol/L, and TAN is the total acid number in mg_{KOH}/g_{sample}.

In house TAN titration was not performed due to the limited amount of sample. The elemental composition of acid mixtures A and B are listed in Table 3. Here it can be seen that the acid mixtures contain almost no nitrogen and a small amount of sulphur. By assuming an overarching raw formula $C_nH_{2n+Z}O_2$ for all acids in the sample the average molecular weight of the acid mixture can be calculated by finding n and Z values which matches the molar ratio between carbon and hydrogen. The percentages of C, H, O indicate an average molecular weight of 373 g/mol for acid mixture A and 395 g/mol for acid mixture B, assuming only monoacids, both of which are lower than the average molecular weights obtained by titration. As will be discussed in section 4.1.2.2, the difference between the molecular weight from titration and elemental analysis could come from pollution by non-acid compounds in the sample. The difference in average molecular weight between the two acids however, is consistent for both methods, i.e. the average molecular weight for acid mixture A is lower than for acid mixture B in both methods.

Table 3 Elemental composition of the extracted crude oil acid mixtures

Element	Symbol	Composition [wt.%] acid mixture A	Composition [wt.%] acid mixture B
Carbon	C	79.5	80.1
Hydrogen	H	11.0	11.2
Oxygen	O	8.5	8.0
Sulphur	S	0.56	0.60
Nitrogen	N	0.09	0.09

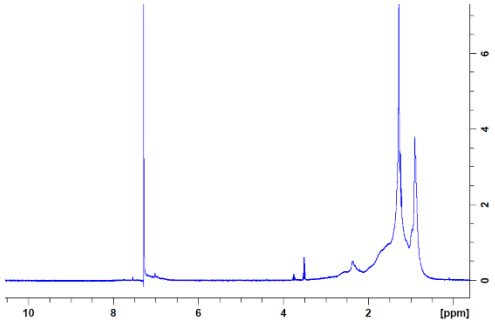

Figure 1 ^{1}H NMR spectrum for the extracted crude oil acid mixture A in $CDCl_3$.

Figure 1 show the ^{1}H NMR spectrum conducted on a 1wt.% solution of acid mixture A. The termination methyl groups give peaks with chemical shifts lower than 1 ppm, while CH_2 methylene bridges have peaks between 1.15 -2.33 ppm [49, 50]. It appears that there are few aromatic groups in the extracted crude oil acid mixture since aromatic groups would register as peaks in the 7-8 ppm range [51]. The absence of aromatic rings is a typical feature of crude oil naphthenic acids [11, 51, 52]. Saab, et al. [51] reported that based on ^{1}H NMR on 1.8% of the analyzed crude oil acids were aromatic. Different theories have been suggested regarding the small amount of aromatic groups found in crude oil acids. Tomczyk, et al. [11] discussed this lack of aromatic acids by suggesting the higher polarity impeded migration from source rock to reservoir. Other authors discuss the role of biodegradation where aromatic hydrocarbons are less susceptible to biodegradation [21, 53]. However, due to their polar nature, aromatic compounds are more prominent in the water phase, Jones, et al. [54] found 30% of oil sands process-affected water (OSPW) acids to have aromatic structures and Stanford, et al. [23], comparing the water soluble acid fractions to the acid fractions of their parent crude oil, found aromatic groups to be more prominent in the water phase acids. Consequently, it is possible that smaller aromatic acids initially present in crude oil were partitioned into the produced water prior to crude oil sampling.

4.1.2. Characterization by GC/MS

4.1.2.1. Assessment of derivatization efficiency

Through GC/MS analysis more information about the acid mixture compositions can be obtained. Published mass spectra of crude oil and bitumen acids reveal broad distributions with a fraction of large and non-volatile molecules [29, 35, 55]. Even If the GC is not able to analyze non-volatile molecules, the use of GC/MS is deemed valid for this work, due to its focus on compounds with partial water solubility, which mainly encompasses smaller acids. The derivatization agent MTBSTFA converts hydroxyl, carboxyl, thiol groups and primary and secondary amines and creates stable ion fragments [M+57], as shown in a previous publication [44], where M is the molecular weight of the acid [56]. For clarity real molecular weight of acids will be denoted g/mol while mass fragments of derivatized acids ([M+57]) will be denoted m/z. The category [M+57] is used to denote all types of derivatized acids, even though molecules with various 1+x functional groups technically becomes a [M+57+x·114] mass fragment. Table S1 in the supplementary material lists the masses for the isomer $C_nH_{2n+Z}O_2$. As explained in section 3.4.2 this table allows the ascertainment of *n* and *Z* from their molecular weight. The average unsaturation for naphthenic acids structures can be described by the double bond equivalent (DBE) as described in Equation 10 [57]. The hydrogen deficiency *Z* is linked to the DBE as described in Equation 11 [58] .

$$DBE = \frac{2C+2-H}{2} \qquad (10)$$

$$Z = -2DBE + 2 \qquad (11)$$

where *C* and *H* are the number of carbon and hydrogen atoms in the formula. Hydrogen deficiency *Z* is used to assign cyclic or aromatic structures due to the absence of alkenes in crude oil [59].

A hydrogen deficiency of -8 or lower in Table S1 could be attributed to either an aromatic ring or a ring structures with 4 rings or more. Aromatic acids have previously been discounted from mass distribution tables like Table S1 [21]. Larger aromatic acids have been reported in both OSPW, crude oil and bitumen [29, 54, 60]. Low molecular weight aromatic acids are however, reportedly not present

in petroleum acid extracts [52], an absence which might be caused by losses to the produced water during production prior to acids being extracted from the crude oil. To cover as diverse a range of carboxylic acids as possible, this article has included aromatic ring combinations to possible acid structures in Table S1.

A previous article [44] discussed the development of the GC/MS method for analysis of naphthenic acid mixtures. Here it was found that all acid structures produced a dominant [M+57] peak. Fatty acids produced the most dominant ion peaks i.e. the low fragmentation, followed by alicyclic and aromatic structures.

4.1.2.2. GC/MS analysis of the extracted crude oil acid mixture

The extracted crude oil acid mixtures were analyzed by GC/MS to give the chromatogram presented in Figure 2. As usual with complex acid mixtures, the GC cannot separate all the molecules present, and the acids elute as an unresolved hump with one mode and few well-defined peaks. The peak at retention time 15 minutes belongs to the internal standard, capric acid. The most distinct peaks at 313 m/z and 341 m/z corresponds to C_{16} and C_{18} aliphatic saturated acids, shown to be respectively palmitic and stearic acids by comparison with the retention time of standard samples. The well-defined peak at 647 m/z at retention time 44 min (C_{40}, Z=-2) gives credibility to the methods ability to analyze relatively high molecular weight molecules. A response factor of 1 was assumed for all acids.

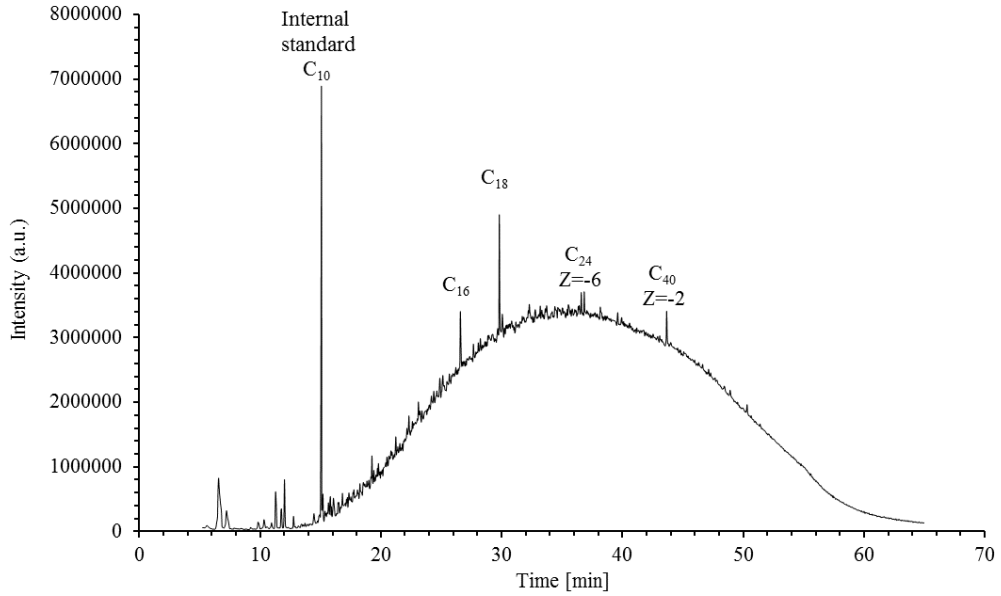

Figure 2 Extracted ion chromatogram of extracted crude oil acid mixture A (159 m/z - 750 m/z). Subtracted by blank solvent chromatogram. The peak at retention time 15 minutes corresponds to the internal standard capric acid C_{10}. Some major peaks listed have stable ion fragments consistent with saturated fatty acids. Their carbon number is indicated on the figure. C_{16} single peak corresponds to palmitic acids, C_{18} single peak correspond to stearic acid, C_{24} double peak is presumed to correspond to a 3 ringed acid, C_{40} single peak is presumed to correspond to an acid with one ring structure. There is an additional 316 m/z specie at the same retention time as C_{40} peak, assumed to be a fragment.

The chromatographic separation in a non-polar column is based on boiling point i.e. the molecular weight. Figure 3 show the elution humps of increasing EIC mass ranges. As the mass of the acids increase they elute successively and with broader peaks due to the increase in possible structural isomer combinations [61]. The EIC mass range 159 m/z - 233 m/z (covering the smallest acids in Table S1) does not have an initial elution hump, but rater present a flat elution from retention time 18 - 60 minutes. These were deemed to be fragments of high molecular weight species and the analysis starts at the next mass range 234-258 m/z or C_{11}. The lack of smaller acids apparent absence of small acid molecules have also been noted previously [19] and can be attributed to pre-sampling production conditions like water-cut and pH. There are also fewer possible structures for lower molecular weight acids as seen in Table S1.

The exclusion of masses below 234 m/z is not enough to remove the influence of fragments. Figure 4 show the EIC for two mass ranges, 234 m/z - 258 m/z and 359 m/z - 383 m/z. Here it can be observed that the small acids after an initial elution hump, reemerge with a flat second elution at a retention time were larger acids elute. It is assumed that the initial elution hump for all EIC mass ranges would represent the actual acids in that range whilst the second and flat elution later in the

chromatogram would be interpreted as fragments of higher molecular weight compounds caused by electron impact ionization or non-acid pollutants. For instance, the acids in the mass range 234 m/z – 258 m/z elute from 12 min - 21 min as seen in Figure 4. After 21 minutes signal responses from this EIC mass range in the chromatogram were disregarded.

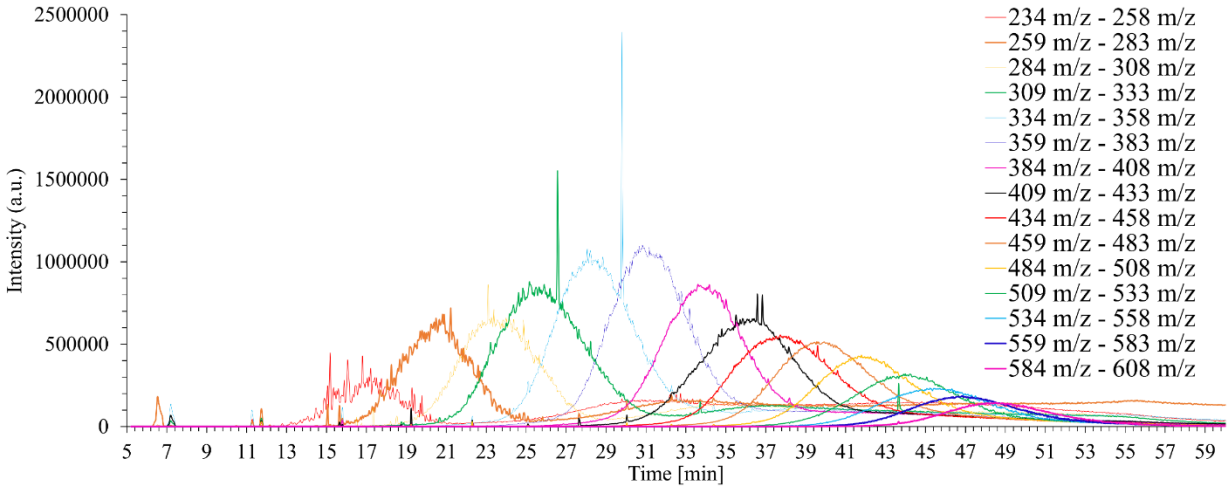

Figure 3 Extracted ion chromatograms (EIC) with increasing mass ranges.

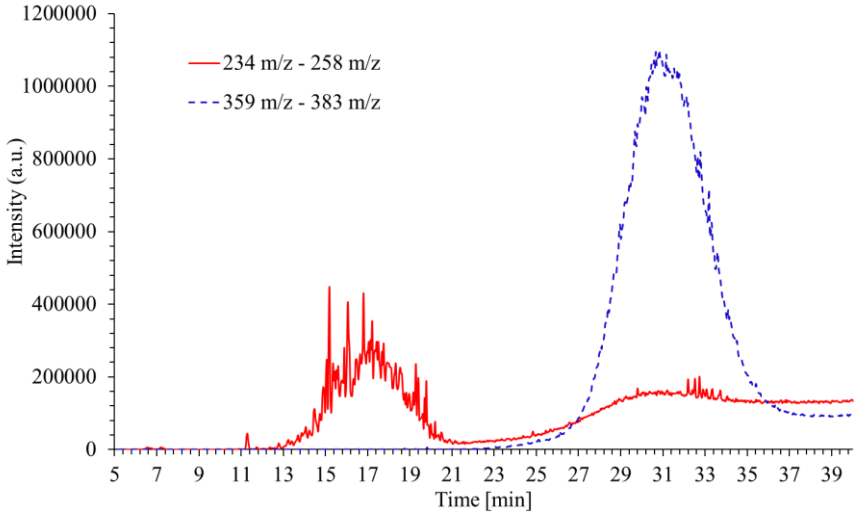

Figure 4 Chromatogram showing response for extracted ion chromatograms (EIC) with mass ranges 234 m/z-258 m/z and 359 m/z-383 m/z. The response of the EIC with mass range 234 m/z-258 m/z from minute 21 is considered as fragments.

Figure 5 displays the mass distribution of the entire elution hump of extracted crude oil acid A. To correct for the bias of fragmentation in the acid distribution the elution humps for different EIC

mass ranges were all given a time segment where the "real" acids elute. Based on these time segments the total chromatogram was split into time segments with increasing minimum m/z cutoff values as shown in Table 4, before the intensity averages of each time segment were normalized by the elution time range and summed up to reconstruct the mass distribution for the whole chromatogram. Consequently, the unwanted fragments are discarded from the distribution. However, this action would skew the reconstructed distribution to higher molecular weight as the false positives for low molecular weight acids are removed. Figure 6 and Figure 7 show the normalized mass distribution for extracted crude oil acid A and B respectively. Compared to the uncorrected distribution for the extracted crude oil acid mixture A shown in Figure 5, many of the registered naphthenic acids with carbon number C_{15} and below are absent in the normalized distribution in Figure 6. As shown previously [44], the higher the molecular weight the more likely it is that a fragment will have high enough mass to register as an acid in Table S1. The extracted crude oil acid mixtures contain many higher molecular weight compounds, which makes them prone to fragmentation bias towards lower molecular weight in this method of low resolution GC/MS and derivatizing with MTBSTFA. Although column bleed should be corrected for through subtracting blank chromatograms and spectra, this method with m/z cutoff also removes the influence of column bleed (207 m/z and 281 m/z for this column) which gets more prevalent at higher temperatures (later retention times).

By applying the time segment method, it is found that 34% of the extracted chromatogram area between 234 m/z and 750 m/z correspond to fragments. When the same method was applied to a commercial acid mixture [44], fragments only comprised 10% of the extracted chromatogram area (209 m/z - 600 m/z). As explained in the same work, fragments with masses high enough to falsely register as [M+57] naphthenic acid masses are more likely obtained with higher molecular weight and more hydrogen deficient (*Z*) acids. As the commercial acid mixture contains lower molecular weight acids with fewer ring structures the difference in fragment area compared to the fragment area obtained with an extracted acid mixture is consistent. The fragment area obtained on extracted acid mixtures is also consistent with the fragmentation observed in mass spectra obtained with model acids [44], where for example the [M+57] peak abundance for: 4-heptylbenzoic acid (C_{14}, Z=-8) was 76%, behenic acid (C_{22}, Z=0) was 80%, and 5β-cholanic acid (C_{24}, Z=-8) was 44%.

Table 4 Table showing how the chromatogram segments were split to ensure that fragments did not skew the mass distribution in favor of lower molecular weight acids

Chromatogram segment	Minimum m/z cutoff
12 min - 21 min	233
21 min - 25 min	258
25 min - 29 min	283
29 min – 32 min	308
32 min – 35 min	333
35 min – 38 min	358
38 min – 40 min	383
40 min – 43 min	408
43 min – 45 min	433
45 min – 48 min	458
48 min – 50 min	483
50 min – 52 min	508
52 min – 54 min	533
54 min – 55 min	558
55 min – 60 min	583

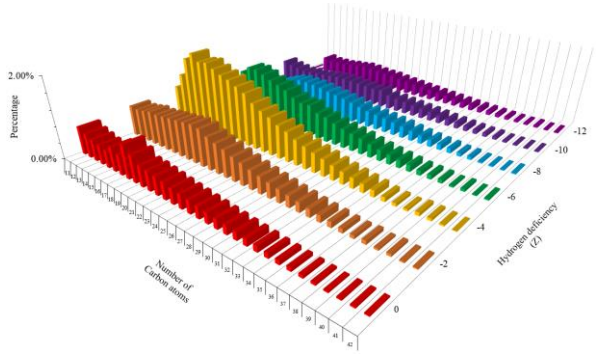

Figure 5 Non normalized mass distribution of extracted crude oil acid mixture A.

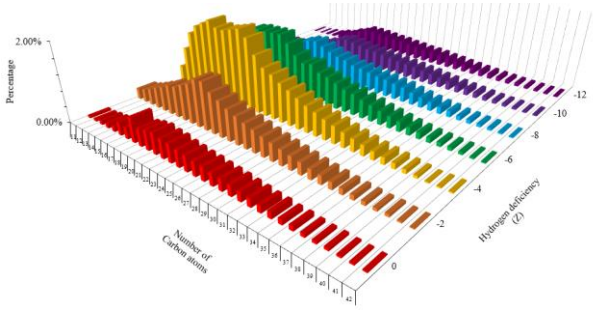

Figure 6 Normalized mass distribution of extracted crude oil acid mixture A. The effect of fragmentation was reduced by splitting up the mass spectrums with different mass range (Table 4) before recombination (see the text for details).

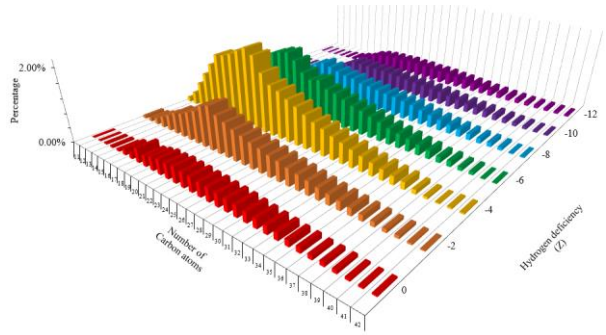

Figure 7 Normalized mass distribution of extracted crude oil acid mixture B. The effect of fragmentation was reduced by splitting up the mass spectrums with different mass range (Table 4) before recombination (see the text for details).

Figure 6 and Figure 7 show that the naphthenic acid mixtures consists of a broad mixture with C_{11}-C_{40} and Z varying from 0 to -12. *Z* = 0 corresponds to aliphatic acids; *Z*-values between -2 and -6 corresponds to alicyclic acids. Finally, a *Z* lower or equal to -8 would indicate the presence of an aromatic ring or an acid with four or more ring structures. Considering the obtained NRM spectrum (Figure 1) indicating an absence of aromatic structures, these acids are most likely alicyclic ring structures with 4-6 rings. Most peaks appear in the C_{13} – C_{27} and 1-3 alicyclic ring range. This is similar to the results obtained by Hemmingsen, et al. [55], who found two ringed acids (*Z* = -4) to be the most abundant in his FT-ICR MS experiments on a North Sea Crude. Qian found three ringed acids (*Z* = -6) to be the most abundant in south American heavy crude. The two mass distributions for the acid mixtures seems to be similar. Clemente, et al. [62] developed

a statistical method to assess the similarities between two naphthenic acid samples by dividing the n, Z distribution into groups of different carbon number ranges. The groups from each acid mixture distribution are then compared with an independent two-sample t-test assuming equal variance. The groups are considered different if the P-value is lower than 0.05. Applying this method to the two distributions indicate there is no significant difference between them (Table S2 in supplementary materials) which is interesting as their parent crude oils come from the same field but from different wells and have different TAN values. This means the two crude oil acids differ by their concentration and not their composition.

From the GC/MS mass distributions the calculated number average molecular weight was 340 g/mol and 360 g/mol for acid mixtures A and B respectively. These numbers are somewhat lower the numbers obtained through elemental analysis, both of which are much lower than the average molecular weight determined by acid number as seen in Table 5. Some explanations could be proposed to explain this difference. The lower average molecular weight obtained through GC/MS was expected due to the inability of the GC to analyze the heaviest acid fraction and lower response factor of higher molecular weight compounds. None of this holds true for the number derived from the elemental composition however, although the calculations are sensitive to measured oxygen content. The number derived from TAN determination is found from the method and equations in the article by Mediaas, et al. [47] (equations 7, 8 and 9). A pollution by non-acid compounds would give an apparent higher molecular weight and provide a possible explanation. This explanation is strengthened by the data obtained in previous work on a commercial acid mixture from Fluka which show that the average molecular weight obtained from all three methods were similar. This would mean that the methodology is correct and that the discrepancy between the method comes from the composition of the extracted acid sample.

Table 5 Summary of results obtained by characterization of the extracted crude oil acid mixtures.

Method	Average molecular weight Acid mixture A [g/mol]	Average molecular weight Acid mixture B [g/mol]
Elemental analysis	373	395
Titration	438*	454*
GC/MS	340	360

**TAN determination performed at Equinor facilities*

4.2. Determination of the partition ratio in presence of monovalent cation

Extracted crude oil acid mixture A in toluene was shaken to equilibrium with aqueous buffers and the separated phases were derivatized and analyzed with GC/MS. The values reported are measured after one day of shaking and it was assumed that equilibrium was reached, although this was not verified. From the total ion chromatogram of the derivatized naphthenic acids, extracted ion chromatograms (EIC) were created with masses between 233 m/z and 700 m/z (from Table S1 the mass range should have been 159 m/z – 700 m/z, however masses which registered as acids below C_{11} were discounted based on their absence in their expected elution time as mentioned in section 4.1.2.2). The area under the chromatogram was used to build calibration curves with the area of the internal standard peak. The calibration curve allows the relationship between the elution area of the internal standard and the elution area of sample to be linked to concentration as shown in Equation 12.

$$\frac{Elution\ area\ acid\ mixture}{Elution\ area\ internal\ standard} = a \cdot \frac{Concentration\ acid\ mixture}{Concentration\ internal\ standard} \qquad (12)$$

where a is the slope between the two fractions. Here concentrations refer to the concentrations of the solutions prior to mixing sample and internal standard together and consequently before

derivatization. This relationship allows unknown concentrations in the oil phase to be calculated with Equation 13.

$$Concentration\ acid\ mixture = \frac{Concentration\ internal\ standard}{a} \cdot \frac{Elution\ area\ acid\ mixture}{Elution\ area\ internal\ standard} \quad (13)$$

For water the procedure is similar, except the volumes used for acidification and organic solvent extraction are taken into account to calculate the concentration in the water after equilibrium partitioning.

Figure 8 show the equilibrium partitioning for the acid mixture. At low pH values all the acids have a low affinity for the water phase. Partitioning starts at pH 7.2 and at the highest pH value, pH 11.5, around 65% of the acids remain in the oil phase. Only 20 % of the total acids seems to end up in the water phase at the highest studied pH value.

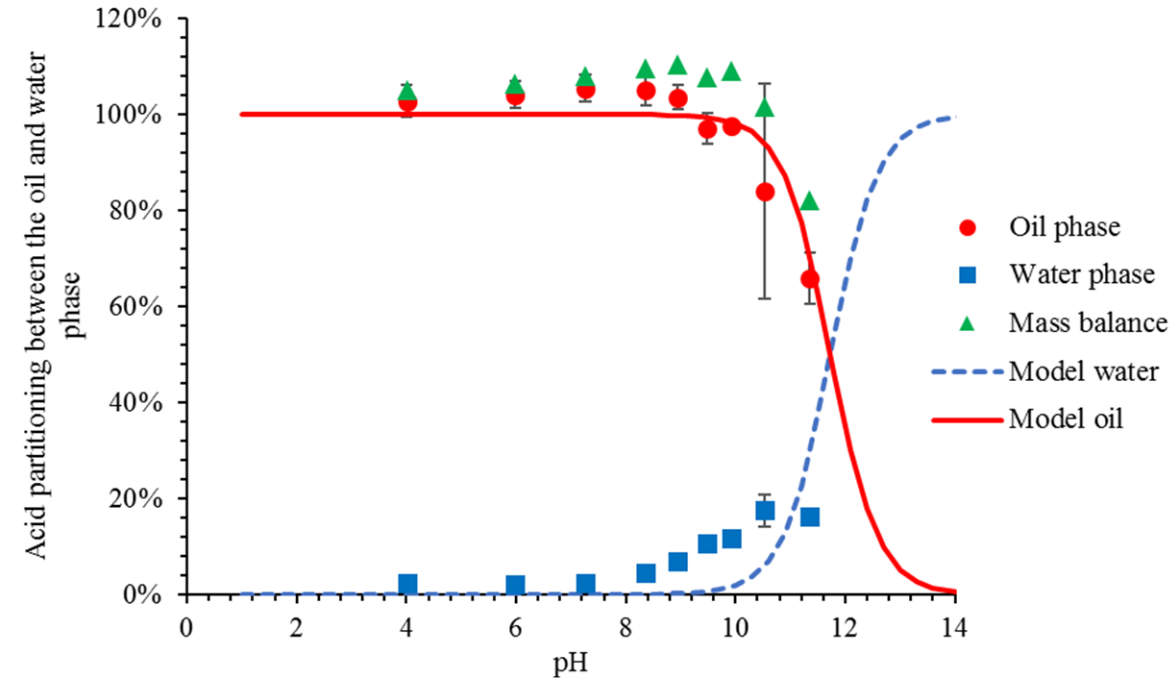

Figure 8 Equilibrium partitioning of the 234 m/z - 700 m/z fraction given as a function of equilibrium pH. Data was fitted with Equations 5 and 6, assuming a single pP_{wo} (pP_{wo}=6.7, pK_a=5). The partitioning was calculated by integrating the entire hump from RT= 12 min to RT= 60 min. The values are the average of two or three measurements where the error bars represent the range of obtained values. Some of the error bars are smaller than the symbols. The mass balance error bars are not shown for clarity.

Previous work on carboxylic acids and naphthenic acids indicates pK_a values between 4 and 6 [30, 63, 64]. From more detailed study of previous research [44] it was concluded that it would be a useful assumption to fix the pK_a in all calculations to a value of 5. The apparent pK_a', i.e. the point where the acid(s) is/are equally distributed between the two phases, equal to the sum of pP_{wo} and pK_a as shown in Equation 14, is used in the text or equations of several authors [43, 45, 65]

$$pK_a' = pK_a + pP_{wo} \qquad (14)$$

From the partitioning of the total acid mixture, a pP_{wo} of 6.7 is calculated by Equations 5 and 6. An apparent pK_a' of 11.7 gives an indication of the small fraction of acids that are able to partition into the water phase. The fit is quite good however, a closer look of the MS data reveals that only the naphthenic acids with a molecular weight lower than 327 g/mol (384 m/z) partition into the aqueous phase. Higher molecular weight naphthenic acids do not significantly partition at pH values lower than 12. It was therefore decided to focus on the lower molecular weight naphthenic acids. The equilibrium partitioning of these naphthenic acids is presented in Figure 9. As expected, these naphthenic acids present a more significant partitioning in aqueous phase than the whole crude oil naphthenic acid mixture. Their equilibrium partitioning could not be fitted with a single partitioning ratio pP_{wo}.

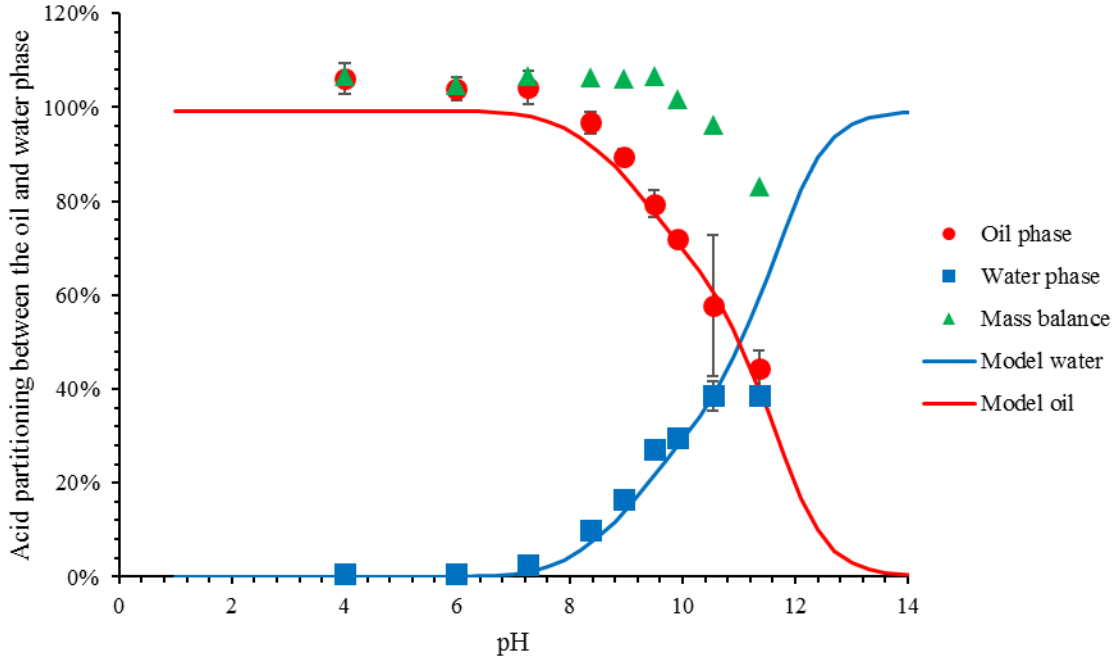

Figure 9 Equilibrium partitioning of the 234 m/z - 383 m/z fraction given as a function of equilibrium pH. Data was fitted with Equations 16 and 17. The values are the average of two or three measurements where the error bars represent the range of obtained values. Some of the error bars are smaller than the symbols. The mass balance error bars are not shown for clarity.

It was decided to divide up the chromatogram into narrower molecular weight ranges using the same method as employed in previous work [44] on a less polydisperse commercial acid mixture. This method will also provide information on the variations of naphthenic acid properties with their molecular weight. Table 6 summarizes the retention times and mass ranges of the different fraction of the chromatogram. This table is consistent with the start of Table 4. The heavier fractions which showed no quantifiable water solubility were disregarded. For every mass range considered in Table 6, a calibration curve was built, normalized by the internal standard. Correlation index r^2 values are also presented in Table 6 (automatically calculated from linear regression fit). In the following sections the partitioning of every mass range is considered and analyzed similarly to the analysis of the commercial acid mixture in Bertheussen, et al. [44].

Table 6 Mass ranges considered for quantitative partition analysis of extracted ion chromatograms(EIC's) of the extracted crude oil acid mixture A and the elution time segment considered to be whole acids and not fragments.

EIC mass fragment range* [m/z]	Integrated time interval of EIC	r^2 linear range 0.66 mM-6.66 mM 0.28 g/L-2.92g/L	Chromatogram area %
234-700	12 min – 60 min	0.998	100%
234-258	12 min - 21 min	0.997	1%
259-283	16 min - 25 min	0.998	3%
284-308	18 min - 29 min	0.999	3 %
309-333	19 min – 32 min	0.999	5 %
334-358	20 min – 35 min	0.999	6 %
359-383	22 min – 38 min	0.999	6 %

*Masses included in the mass ranges are based on naphthenic acid masses [M+57] from Table S1 including their isotope [M+57]+1.

The areas used for concentration determination for the different fractions encompassed 24% of the total chromatogram area spanning from 234 m/z to 700 m/z. The remaining 76% correspond to higher masses than 383 m/z (42%) which were not included due to their negligible water partitioning and non-included fragment humps (34%) as described in section 4.1.2.2.

Figure 10a and Figure 10b show the equilibrium partitioning of the mass ranges 234 m/z - 258 m/z and 259 m/z -283 m/z, corresponding to C_{11}/C_{12} and C_{13}/C_{14} acids respectively as seen in Table S1. The EIC intensity of this fraction comprises 1% of the total chromatogram area. The acids in the 234 m/z - 258 m/z mass range are completely oil-soluble below pH 6 and has an almost complete transfer to the water phase from pH 6 to 10. Equations 5 and 6 gives an adequate fit with the data when the pP_{wo} is 3.0, indicating that the molecular weight range is narrow enough to be modeled by a single pP_{wo}. This is confirmed by the R^2 values calculated from Equation 15 [66, 67] and reported in Table 7.

$$R^2 = 1 - \frac{\sum(y - y_{fit})^2}{\sum(y - y_{avg})^2} \qquad (15)$$

Here R^2 is the correlation index, y is the data point, y_{fit} is the calculated value from the fitted curve and y_{avg} is the arithmetic average of all y data points. The apparent pK_a' indicates a phase

transfer from pH 8.0. The EIC intensity of the 259 m/z -283 m/z mass range fraction comprises 3% of the total chromatogram area. Equations 5 and 6 give a good fit with the data when the pP_{wo} is 3.8 (higher than the value found for the mass range 234-258 m/z) which indicates a phase transfer at the apparent pK_a' of 8.8.

The equilibrium partitioning of the mass ranges 284 m/z -308 m/z and 309 m/z -333 m/z are shown in Figure 10c and Figure 10d. These mass ranges correspond to C_{15}/C_{16} acids and C_{17} acids respectively and likewise comprise 3% and 5% of the total chromatogram area. A pP_{wo} of 4.6 is obtained for the mass range 284 m/z -308 m/z, giving an apparent pK_a' of 9.6 as seen in Figure 10c. For the mass range 309 m/z -333 m/z, the obtained pP_{wo} is 5.8 indicating a phase transfer (apparent pK_a') at pH 10.8.

Figure 10e and Figure 10f show the equilibrium partitioning of the mass ranges 334 m/z -358 m/z and 359 m/z -383 m/z. These mass ranges correspond to C_{18}/C_{19} acids and C_{20}/C_{21} acids respectively and both comprise 6% of the total chromatogram area. Due to the incomplete partitioning, Equations 5 and 6 do not give a good fit. with the data for these two higher mass ranges, consistent with the R^2 values seen in Table 7. The obtained pP_{wo} values of 6.7 and 6.8 respectively does not accurately predict the system behavior at high pH.

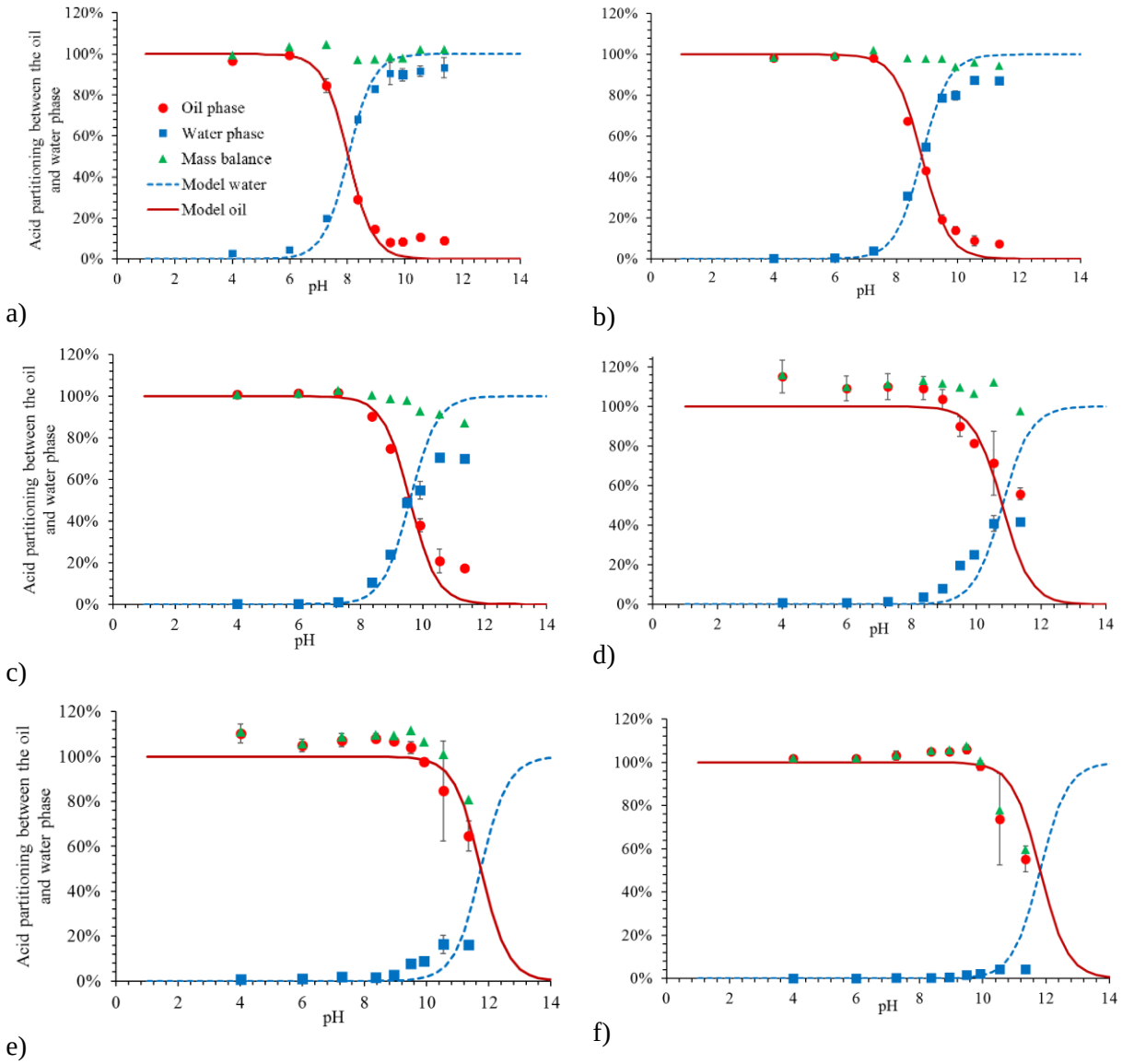

Figure 10 Equilibrium partitioning of the naphthenic acid mass fractions, of the extracted crude oil acid mixture A, given as a function of equilibrium pH. a) 234 m/z - 258 m/z, b) 259 m/z -283 m/z, c) 284 m/z -308 m/z, d) 309 m/z -333 m/z, e) 334 m/z -358 m/z, f) 359 m/z -383 m/z. Data was fitted with Equations 5 and 6, assuming pK_a=5, and a single pP_{wo}, a) 3.0, b) 3.8, c) 4.6, d) 5.8, e) 6.7, f) 6.8. The values are the average of two or three measurements where the error bars represent the range of obtained values. Some of the error bars are smaller than the symbols. The mass balance error bars are not shown for clarity.

As can be seen the mass balance determined for all the systems in Figure 8 and Figure 10 are generally close to 100%. One exception comes when higher molecular weight acids partition at high pH (Figure 10e and Figure 10f). Here the mass balance is lower, most likely caused by the light brown colored layer in the water phase at the centrifugation tube wall after centrifugation for experiments with initial pH 11 and 12 (pH_f=10.4 and 11.4). It was impossible to improve the separation. This trend was also observed for high acid molecular weights at high pH in previous

work [44]. This loss of sample was attributed to the precipitation of sodium salt of naphthenate. The precipitation is only significant for the highest molecular weight acids in their carboxylate form as noticed previously. It can be noticed in Figure 8, 10d and 10e that the mass balances are slightly higher than 100%. This is most likely due to uncertainties in the different steps of the analysis like calibration curve buildup, water phase extraction and mass determination. The error bars presented in the different figures concern the reproducibility of the experiments.

Higher mass ranges (above 383 m/z), which corresponds to 42% of the total chromatogram area, does not have sufficient partitioning to the water phase to be considered with this method. The concentration of the water-soluble fraction of naphthenic acid in oil and water can be determined by the sum of every individual fraction in proportion to their ratios of the total water-soluble fraction chromatogram (24% for masses 234 m/z – 383 m/z) as seen in Equation 16 and 17. Here the ω_i and $P_{wo,acid,i}$ are the chromatogram area fraction and partition ratio for each mass range respectively.

$$[HA]_{w,tot} = \sum_{i=1}^{n} \omega_i \frac{[HA]_{o,init}}{\frac{[H^+]}{P_{wo,acid,i}(K_{a,HA}+[H^+])}+\frac{V_w}{V_o}} \qquad (16)$$

$$[HA]_{o,tot} = \sum_{i=1}^{n} \omega_i \frac{[HA]_{o,init}}{1+\frac{V_w P_{wo,acid,i}(K_{a,HA}+[H^+])}{V_o[H^+]}} \qquad (17)$$

Figure 9 shows the summation model of the water-soluble fraction of the extracted crude oil acid mixture A. It can be seen that the model gives a good fit to the data.

A summary of the partitioning results for the extracted crude oil acid mixture A, are summarized in Table 7. The pP_{wo} and consequently the apparent pK_a' increases with the acid mass.

Table 7 Mass ranges and equivalent molecular weight shown in a summary along with their respective pP_{wo} calculated by imposing pK_a =5 in Equations 5 and 6. The area fraction of the elution hump of each mass range is also indicated. pK_a = 5 imposed for naphthenic acids in all mass ranges.

Mass range	Molecular weight	Approximate carbon numbers	pP_{wo}	Chromatogram area %	pK_a'	R^2 Oil phase	R^2 Water phase***
234 – 258 m/z	177 – 201 g/mol	C_{11}/C_{12}	3.0	1 %	8.0	0.98	0.97
259 – 283 m/z	202 – 226 g/mol	C_{13}/C_{14}	3.8	3 %	8.8	0.99	0.96
284 – 308 m/z	227 – 251 g/mol	C_{15}/C_{16}	4.6	3 %	9.6	0.97	0.85
309 – 333 m/z	252 – 276 g/mol	C_{17}	5.8	5 %	10.8	0.86	-0.01
334– 358 m/z	277 – 301 g/mol	C_{18}/C_{19}	6.7*	6 %	11.7	0.92	-0.80
359– 383 m/z	302 – 326 g/mol	C_{20}/C_{21}	6.8*	6 %	11.8	0.94	-14.76
>384 m/z	>327 g/mol			42 %	-	-	-
234-700 m/z	177-643 g/mol		6.7	100%**	11.7	0.98	-2.30

*pP_{wo} calculated on incomplete partitioning in water at high pH. ** Elution hump area do not add to 100% due to non-included fragment areas as can be seen in Figure 4. ***low degree of partitioning makes the denominator of the fraction term in Equation 15 small, which gives low or negative R^2 values.

Figure 11 show the linear relationship of the cologarithm of the partition ratio as a function of molecular weight obtained for the extracted crude oil acid mixture A and previously obtained results for a commercial acid mixture from Fluka [44]. In this article we have assumed a pK_a of 5, based on previous works [30, 63, 64]. Even if this value seems the most likely, we have conducted a small sensitivity analysis on the influence of pK_a on pP_{wo} on the data in Figure 10a. When the pK_a is increased or decreased with 1, the pP_{wo} decreases or increases with 1 respectively. The shape or location of the predicted oil and water concentration curves in Figure 10a are also unchanged by a change in the assumed pK_a.

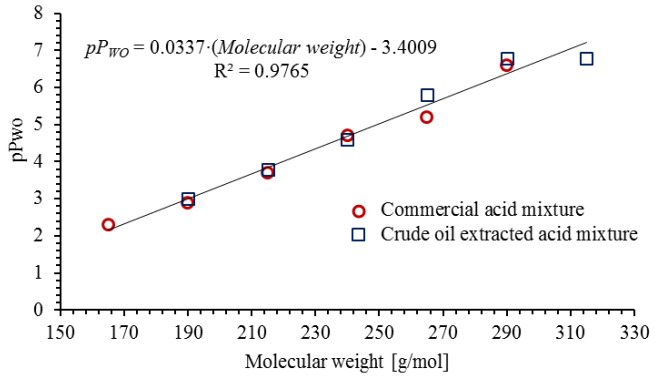

Figure 11 Graph indicating the linearity of the cologarithm of the partition ratio pP_{wo} of acid mass ranges from the NA mixtures based on molecular weight. Commercial acid mixture data from [44]. The molecular weight indicated corresponds to the middle of the mass ranges.

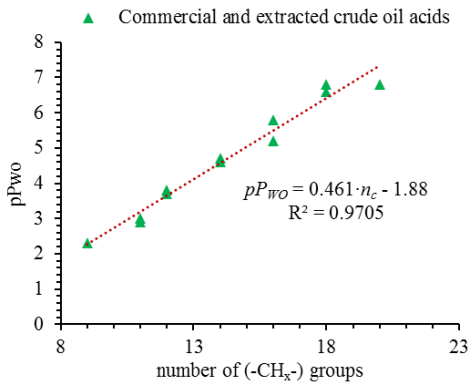

Figure 12 Graph illustrating the link between obtained partition ratio results for a commercial acid mixture [44], extracted crude oil acids and Equation 18.

4.3 Discussion about partition ratio variation with molecular weight

4.3.1 Thermodynamic explanation

Over the years libraries of partition coefficients have been gathered [68] and different models has been used to estimate the partitioning behavior of molecules based on structure [69]. Although the most widely used partition coefficient, $\log P_{octanol}$, refers to an octanol-water system, Leo, et al. [68] also presented solvent correlation to correct for partitioning coefficients between different solvents. Most of these models are dependent on more structural information [70] than what can be obtained through the molecular weight alone due to the impressive number of structural isomers encountered in organic molecules. It should be mentioned that $\log P_{toluene}$ is equal to the pP_{wo} used in this work.

Data from Figure 11 allows the determination of some thermodynamic parameters characterizing the partitioning of naphthenic acids between aqueous solution and toluene.

Cratin [71] demonstrated Equation 18 which presents the variation of the partitioning ratio with the carbon number of homologue series.

$$pP_{wo} = \frac{n\Delta\mu_{L(-CH_x-)}}{2.3RT} + \frac{\Delta\mu_{H(-COOH)}}{2.3RT} + \log\frac{\overline{V}_w}{\overline{V}_o} \qquad (18)$$

Where $\Delta\mu_{L_{(-CH_x-)}}$ stands for the free energy change of one lipophilic group of a molecule when the transfer occurs from oil to water. $\Delta\mu_{H_{(-COOH)}}$ stands for the free energy contribution of the hydrophilic group of the molecule when the transfer occurs from oil to water. n stands for the number of lipophilic groups. $\bar{V}_o$ and $\bar{V}_w$ are the molar volumes of the solvent and water. R and T are the ideal gas constant and the temperature. Figure 12 shows how the number of lipophilic groups increase the pP_{wo} of crude oil acids.

From the slope of 0.461 the free energy change per mole of methylene group $\Delta\mu_{L_{(-CH_x-)}}$, when the molecule is transferred from oil to water and the temperature is set to 25 °C, can be calculated to 2.63 kJ/mole. The positive number indicates that this group spontaneously partitions into the oil phase as expected. From the intercept the contribution for the chosen hydrophilic group $\Delta\mu_{H_{(-COOH)}}$ can be calculated by using molar volumes for toluene and water to be -6.3 kJ/mole.

A value of the free energy change during water to heptane partition for some long chains saturated, linear fatty acids of 3.5 kJ/mole of CH_2 group has been determined by Mukerjee [72]. This value is significantly higher than the one determined in the present study, even if Mukerjee [72] has noticed that the value decreases for the longest tested acids. Two reasons can be pointed out to explain this difference. First, the difference of polarity between the oil phases used in the two study (heptane vs. toluene). Second, the presence of cycloalkyle rings in the commercial and crude oil naphthenic acid mixtures. These differences are consistent with a lower $\Delta\mu_{L_{(-CH_x-)}}$ compared with the system considered by Mukerjee [72].

Another interesting comparison to be performed is between oil-water partition coefficient and micellization. The free energy contribution per each CH_2 group is generally considered to be -3.0 kJ/mol [73, 74]. The difference with the CH_2 group contribution for the partition of naphthenic acid found in this article is mostly due to the same factors as previously mentioned i.e. oil phase polarity and presence of cycloalkyle rings in the naphthenic acid structure.

4.3.2 Comparison with model acid 4-heptylbenzoic acid

In previous work [43] the partitioning of the model acids phenyl acetic acid and 4-heptylbenzoic acid between heptane and 3.5% NaCl water was mapped over the pH range. The small acid phenyl

acetic acid was found to be almost completely water soluble even at low pH values and does not lend itself to comparative observations. The larger 4-heptylbenzoic acid had a sharp phase change around pH 8 (*pKa'*). As discussed in previous work [44], 4-heptylbenzoic acid would give a stable ion mass fragment covered by the mass range 259 m/z – 283 m/z. This mass range indicated a phase change at the apparent pK_a' of 8.7 for the commercial acid mixture and 8.8 for the extracted crude oil acids A. However, partitioning in [43] was measured using heptane as the oil phase. To have a meaningful comparison, experiments were repeated in toluene. When 4-heptylbenzoic acid is partitioned in toluene as seen in Figure 13, Equations 5 and 6 gives a pP_{wo} is 3.8, apparent pK_a' of 8.8 which overlaps perfectly with the partitioning from the mass range 259 – 283 m/z in the two acid mixtures. The figures also show the influence of the solvent on the pKa': the partition takes place at a lower pH when the polarity of the organic solvent is lower. We can also notice that the partition curve of 4-heptylbenzoic acid in toluene is well-fitted by equations 5 and 6 contrary to heptane. Other equilibria, not taken into account by the model presented in section 2.2, might have an influence in heptane.

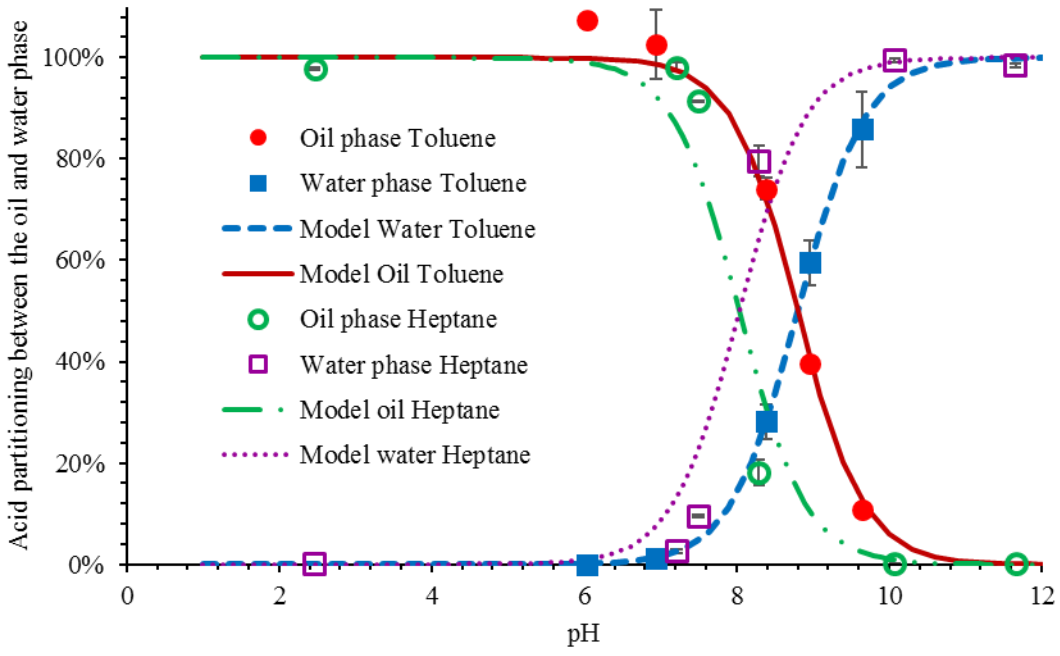

Figure 13 Equilibrium partitioning of 4-heptyl benzoic acid given as a function of equilibrium pH. The system had initial concentration of 1 mM acids in toluene or heptane with aqueous buffer (3.5 wt.% NaCl). Data was fitted with Equations 5 and 6. (pP_{wo}=3.43, pK_a=4.6 for heptane, pP_{wo}=3.8, pK_a=5 for toluene). Heptane data taken and replotted from Bertheussen, et al. [43]. The values are the average of two measurements where the error bars represent the range of obtained values. Some of the error bars are smaller than the symbols.

4.3.3 Comparison of partition ratio with literature

Zhang, et al. [75], using HPLC ESI/HRMS, reported octanol−water distribution ratios, D_{ow}, for carboxylic acids from OSPW with increasing carbon number. It is interesting to note a large change in partitioning with structure having increasing DBE number in the work of Zhang, et al. [75]. In order to compare results from different studies, the reported data were converted into pP_{wo} in toluene and the structure characterized by n_c and Z with the following relationships: data reported in octanol were calculated in toluene according to the relationship by Leo, et al. [68], $\log P_{toluene} = 1.135 \log P_{octanol} - 1.777$, distribution ratios were converted into partition ratios with equation 9 in Bertheussen, et al. [43] and DBE values are converted to Z number through Equation 11. As explained in section 4.3.1, $\log P_{octanol}$, commonly refers to an octanol-water system. $\log P_{toluene}$ describes the partition coefficient using toluene as the organic solvent instead of octanol.

Experimental data are first compared and can found in Table 8. In general the estimated numbers from Zhang, et al. [75], differ from the ones obtained for the acid mixtures analyzed in work. Even the most hydrophobic structures reported (Z=-4), appears with pP_{wo} 1-2 orders of magnitudes lower, indicating an overestimated water solubility. An argument could be made for the difference in source material. Extracted crude oil acids from a crude oil which has been in contact with water as done in this work, could contain different acid structure isomers compared to oil sands process-affected water (OSPW), as shown by the experiments by Stanford, et al. [23].

Havre, et al. [30] studied naphthenic acid equilibrium partitioning between a 2wt.% acid content crude oil and aqueous buffers using GC/MS. Reported values for naphthenic acid partitioning is listed in Table 8. As a pK_a of 4.9±0.1 was given for the acids, this value was used to calculate the pK_a' values. It should be mentioned that the partition ratio in this instance was between crude oil and water, which is compared to pK_a' values obtained with partition ratio between toluene and water. Crude oil is a different matrix with thousands of different saturates and aromatics, in addition to the presence of asphaltenes. Despite this limitation, the reported values are very similar to the ones obtained in this work for the acids listed in Table 8. This speaks to the applicability of the obtained results and method to describe crude oil acid mixture behaviors for all crude oils. The data obtained by Havre, et al. [30] show the influence of the number of alicyclic structures (Z) at similar carbon number: The higher the carbon number the lower the pP_{wo} . The values obtained in

the present study are average data for given mass ranges and the influence of *Z* on the partitioning is therefore not visible.

Celsie, et al. [32] used COnductor-like Screening MOdel for Realistic Solvents (COSMO-RS) to model how pH would affect naphthenic acid concentrations in water for 55 representative naphthenic acids. Scarlett, et al. [76] reported the partitioning for organic acids based on quantitative structure activity relationship (QSAR) models. A comparison between simulated data and experimental data for some acids is shown in Table 8. All simulated data have been corrected for $\log P_{octanol}$ to $\log P_{toluene}$. In general, the data simulated with COSMO-RS predict a more conservative water concentration while the data obtained with QSAR predict higher acid water solubility compared to the experimental data obtained in this work. In addition, COSMO-RS data assumes no salt in the water phase. From the salting out effect [77], one would assume salinity would decrease the partitioning which was shown by Celsie, et al. [32] who calculated that salinity decreases the partitioning of naphthenic acids slightly. This was also demonstrated on the synthetic and complex tetraacid BP10 [78], made to mimic the properties of the ARN acid, where the partitioning coefficient K_{wo} between chloroform and water decreased when salinity increases.

Table 8 Table comparing apparent pK_a' values for carboxylic acids calculated from simulated data, COSMO-RS by Celsie, et al. [32], QSAR by Scarlett, et al. [76] and experimental values from this work and calculated values from experimental data reported by Havre, et al. [30] and Zhang, et al. [75]. LogP values have all been converted from octanol to toluene using the correlation by Leo, et al. [68] $logP_{toluene} = 1.135 logP_{octanol} - 1.777$. $logP_{toluene}$ is equal to pP_{wo}.

Acids			Apparent pK_a' values where phase transfer between oil and water would occur				
			Simulations		Experimental		
Carbon number	Hydrogen deficiency Z-value	Molecular weight [g/mol]	COSMO-RS ** [32]	QSAR* [76]	Acid mixtures toluene/water partitioning***	Crude oil/water partitioning [30]****	OSPW, PDMS partitioning [75]*
C_{10}	Z= 0	172.3	8.5	7.7	7.3	-	-
	Z=-4	168.2	7.1	6.4		7.0	-
C_{11}	Z=-2	184.3	11.4	7.6	8.0	7.4	-
	Z=-4	182.3	8.5	6.8		7.3	-
C_{12}	Z=-4	196.3	8.8	7.3		7.9	6.6
C_{13}	Z=-4	210.3	12.2	7.9	8.8	8.5	6.7
C_{14}	Z=-6	222.3	8.8	7.9		8.5	6.7
	Z=-0	228.4	-	10.45	9.7	-	-
C_{16}	Z=-6	250	11.6	-		9.6	7.2
C_{18}	Z= 0	284.5	-	12.0	11.7	-	-

*As only log(P) was reported the pK_a was assumed 5 for all acids. **Some reported pK_a values are much higher than 5, giving high apparent pK_a' values. ***Average of results for matching naphthenic acid mass range obtained in this work and previously obtained results on a commercial acid mixture [44] as referenced in Figure 11. ****Used reported pK_a value of 4.9 for all reported partition ratios by Havre; due to the use of crude oil as oil phase solvent, no logP solvent correction was attempted.

4.3. Influence of divalent cation on partitioning

Adding a divalent cation like calcium to the water phase can affect the partitioning of naphthenic acids as seen in previous work for model acids [43] and a commercial acid mixture [44]. In the case of model acids; calcium only affected the larger of the two acids, 4-heptylbenzoic acid, by forming calcium salt that precipitated at pH values over 7. The smaller of the two acids tested, phenylacetic acid, was not affected. A similar trend was seen for the commercial acid mixture from Fluka for acids with 13 or more carbon atoms, but the mechanism was different: Instead of being due to the formation of insoluble calcium naphthenate, the difference was shown to be caused by the formation of oil-soluble calcium naphthenate. This phenomenon was previously mentioned in the literature [31, 39, 79]. To map how calcium would affect an acid mixture extracted from crude oil, the same experimental setup presented in section 4.2 was repeated with the difference that 10 mM $CaCl_2$ was added to the water phase. This concentration is much smaller than the NaCl

concentration (~600 mM) and therefore the total ionic strength is similar to previous experiments without calcium. Another difference was that the final pH 11 was obtained through pure NaOH addition instead of the bicarbonate buffer due to $CaCO_3$ incompatibility. As mentioned the separated water phases from the experiments with the two highest pH values in section 4.2 in absence of $CaCl_2$, had a light brown colored layer along the tube wall in the water phase indicating the presence of particles. No such layer was observed in the partitioning experiments with calcium. The same effect was also observed for the commercial acid mixture [44]. The overall effect of calcium on the whole acid mass range is shown in Figure 14. Here it can be observed that at high pH, calcium has an effect on the partitioning. Due to the low degree of overall partitioning for the crude oil acid mixture, trends are not as well defined. Better mass balances are also obtained when calcium is present, likely due to the clear oil and water phase obtained after centrifugation and no light brown layer.

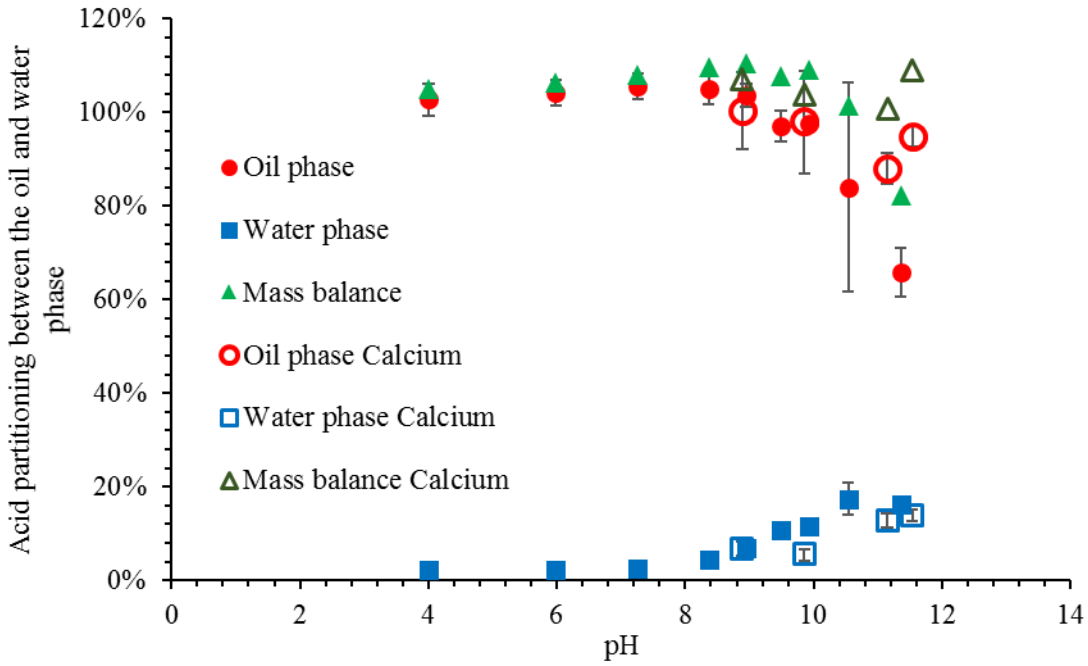

Figure 14. Equilibrium partitioning of the 234 m/z - 700 m/z fraction given as a function of equilibrium pH. The values are the average of two or three measurements where the error bars represent the range of obtained values. Some of the error bars are smaller than the symbols. The mass balance error bars are not shown for clarity.

The mass ranges were evaluated individually as was done previously in section 4.2. Figure14a show the partitioning of the acids in the mass range 234 m/z - 258 m/z (C_{11}/C_{12}) in comparison

with the partitioning in the system without calcium. As indicated by the similar partitioning, smaller acids are largely unaffected by the presence of calcium in the water phase, as was the case for the same acid fraction of a commercial acid mixture [44] and the small model acid phenylacetic acid [43]. Figure 14b compares the partitioning of the mass range 259 m/z – 283 m/z (C_{13}/C_{14}). Here it can be observed that in the system with calcium the partitioning is reduced at pH values higher than pH 9. The large model acid 4-hepylbenzoic acid, falls into this mass range.

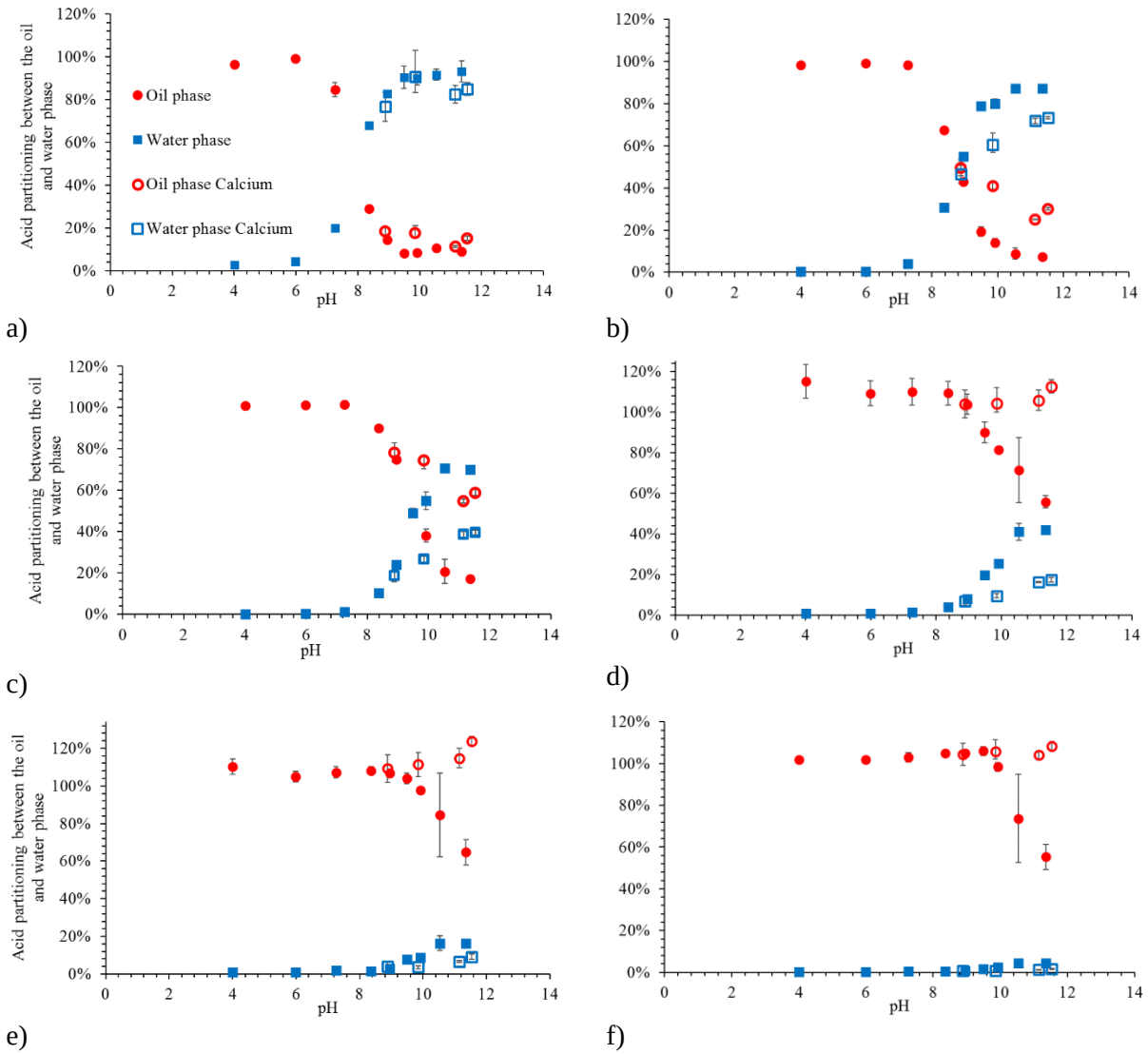

Figure 15 Equilibrium partitioning of the naphthenic acid mass fractions, of the extracted crude oil acid mixture A, given as a function of equilibrium pH. a) 234 m/z - 258 m/z, b) 259 m/z -283 m/z, c) 284 m/z -308 m/z, d) 309 m/z -333 m/z, e) 334 m/z -358 m/z, f) 359 m/z -383 m/z. The values are the average of two or three measurements where the error bars represent the range of obtained values. Some of the error bars are smaller than the symbols. For the sake of clarity, figures without mass balances are presented here, and figures with mass balances are presented in the Supporting Information.

The acid partitioning with and without calcium present for the remaining mass ranges 284 m/z - 308 m/z (C_{15}/C_{16}), 309 m/z - 333 m/z (C_{17}), 334 m/z - 358 m/z (C_{18}/C_{19}) and 359 m/z – 383 m/z (C_{20}/C_{21}) is shown in Figure 14 c-f. Here the same trend as shown before prevails. At pH 9, calcium does not affect the partitioning, while at higher pH values the partitioning is reduced as the molecular weight of the acids increases. The mass balances are close to 100%, which indicate little or no loss of sample, such as precipitation of calcium naphthenate particles, as confirmed by visual inspection of the samples after centrifugation. Overall these results are in good agreement with results obtained in previous work on a commercial acid mixture, where it was concluded that at high pH and in the presence of calcium, there is formation of oil-soluble calcium naphthenates. The tendency for calcium to form calcium naphthenate with higher molecular weight acids has been reported previously [79].

To learn more about the content of the oil phase after partitioning, a high-volume experiment was performed followed by elemental analysis of the oil phase.
Due to the limited amount of sample, only one parallel was performed on the extracted crude oil acid mixture B. The results are considered representative for values obtained with the extracted crude oil acid mixture A, due to the statistically insignificant mass distribution difference between them.

Previous results with a commercial acid mixture [44] showed that after partitioning with calcium present the elemental composition remained unchanged at pH 2, while at pH 10 and 11.5 the amount of oxygen was reduced by a factor of 2, indicating an increase in molecular weight for the acids remaining in the oil phase, in agreement with the relationship between pP_{wo} and molecular weight seen in Figure 11. Regarding calcium, there was none present in the oil phase at pH 2, while at the higher pH values calcium was present in a calcium to O_2 ratio of 0.25 for pH 10 and 0.5 for pH 11.5. The calcium to O_2 ratio show how many of the carbonyl groups are bound to calcium in the oil (note that 2 $RCOO^-$ are needed per Ca^{2+}).

Comparing the previously obtained results with the commercial acid mixture with the results obtained with the extracted crude oil acids it can be observed in Table 9 that the oxygen content is

half of its original value for the extracted crude oil acids as well. This result was surprising as in contrast to the commercial acid mixture only a small fraction of the total acids of the extracted crude oil acid mixture partition over to the water phase at high pH, as seen in Figure 14. The calcium to O_2 ratio for the extracted crude oil acids at high pH are around 0.5, the same ratio as obtained for the commercial acid mixture, indicating that all the available carboxyl groups in the oil phase are bound to calcium. This result is also surprising, as it seems that even the largest acids have dissociated and formed oil-soluble calcium naphthenates.

Studies by Havre [34] concluded that calcium naphthenate is not formed in the water phase, rather they are formed through interfacial reactions between calcium and dissociated carbonyl groups as discussed by Brandal [35]. At final pH 11.5 the elemental composition indicates an average acid carbon number of C_{46} and molecular weight 669 g/mol. This molecular weight is not initially present in the naphthenic acid sample (Figure 7) and indicates that our calculation most likely does not capture some of the reaction happening in the presence of calcium. Consequently, more analyses are required to fully understand the mechanism in presence of calcium.

Table 9 Elemental composition of evaporated oil phase acids after shaken to equilibrium with pH 12 buffer with 3.5% NaCl and 10 mM $CaCl_2$.

Final pH	**Carbon [%]**	**Hydrogen [%]**	**Oxygen [%]**	**Calcium [%]**	**Sodium [%]**	**Chlorine [%]**	**Mol $\frac{\text{Calcium}}{\text{Mol } O_2}$**
pH 11.5	78.4	11.5	4.51	3.0	0.03	<0.4	0.53

In summary it appears that results obtained with an extracted crude oil acid mixture are similar to the ones found with a commercial acid mixture. Calcium reduces the high pH partitioning of C_{13}-C_{19} acids through the formation of oil-soluble calcium naphthenate, while the smaller acids are seemingly unaffected by calcium.

5. Conclusion

This article has continued and expanded previous work, detailing the equilibrium partitioning of a commercial acid mixture, by investigating the equilibrium partitioning of an extracted crude oil acid mixture. Two extracted crude oil acid mixtures from the same field were characterized and found to have statistically insignificant differences in mass distributions, even though their corresponding crude oils presented very different TAN values. A mass distribution bias for the GC/MS analysis method was corrected for and the acid mass distributions obtained reveal broad structural distributions consisting mainly of saturated ring structures with 2 to 3 rings. The partitioning of the extracted crude oil acid mixture A as a function of pH was analyzed with GC/MS. Only the acids with carbon numbers lower than C_{22} partitioned to the water phase over the pH range 7-12. To be able to model the partitioning with a single partition ratio, P_{wo}, the acid mixture analysis was split up into narrower molecular mass ranges with a width of 25 g/mol. Summing up normalized contributions from each mass range, a partitioning curve for the whole water-soluble acid mixture fraction was established. Partition ratios obtained in this work have a complete overlap with previously obtained partition ratios using a commercial acid mixture. The influence of solvents on partitioning was discussed and, through solvent correction factors, previously reported partitioning results, both experimental and simulated, were compared to results obtained in this work. Calcium affected the high pH partitioning of larger acids, while smaller acids were unaffected. Oil phase analysis indicate that all remaining oil phase carboxylic groups are bound to calcium. Results indicate some universal properties for crude oil acids.

Acknowledgements

This work was carried out as a part of SUBPRO, a Research-based Innovation Centre within Subsea Production and Processing. The authors gratefully acknowledge the financial support from SUBPRO, which is financed by the Research Council of Norway, major industry partners and NTNU. The authors would like to thank Einar Eng Johnsen (Equinor) and Hege Kummernes (Equinor) for providing the North Sea naphthenic acid samples, Gunhild Neverdal (Equinor) for GC/FID analysis and Bicheng Gao (NTNU) for the determination of NMR spectrum. The naphthenic acid extraction was performed at Equinor Research Centre Trondheim.

Supporting information. Table S1 displaying the naphthenic acid masses for increasing carbon numbers and hydrogen deficiencies. Table S2 displaying the details in the statistical comparison t-test between the two naphthenic acid mixtures. Figure S1 a-f, graphs showing equilibrium partitioning of naphthenic acids with and without calcium and the mass balances.

References

1. Warner, R., Western European refineries and acidity in crude oil. In S&P-Global-Platts-Oil, Ed. S&P Global Inc: New York, USA, 2017; pp 1-6.
2. Prescott, C. N., Subsea Separation and Processing of Oil, Gas & Produced Water. Past, Present and Future. Why We Need It Now. In *Rice Global E&C Forum*, Fluor Offshore Solutions: Houston, Texas, 2012.
3. Berntsen, J. S., Qualified technology (TRL 5) to remove produced water, at seafloor or topside, before it becomes difficult to treat. In *Tekna Produced Water Management Conference*, 24th-25th January, Stavanger, Norway, 2018.
4. Shaiek, S.; Laurent, G., SpoolSep for Subsea Produced Water Separation, OTC-25934. In *Offshore Technology Conference*,, 4-7 May, Houston, Texas, USA 2015.
5. Ligiero, L. M. Crude oil/water interface characterization and its relation to water-in-oil emulsion stability. University of Pau and Pays de l'Adour (UPPA), Pau, France, 2017.
6. Flesisnki, L. Étude de la stabilité des émulsions et de la rhéologie interfaciale des systèmes pétrole brut/eau: Influence des asphaltènes et des acides naphténiques. University of Pau and Pays de l'Adour (UPPA), Pau, France, 2011.
7. Dudek, M.; Bertheussen, A.; Dumaire, T.; Øye, G., Microfluidic tools for studying coalescence of crude oil droplets in produced water. *Chemical Engineering Science* **2018,** 191, 448-458.
8. Headley, J. V., McMartin, Dena W., A Review of the Occurrence and Fate of Naphthenic Acids in Aquatic Environments. *Journal of Environmental Science and Health Part A* **2004,** A39, (8), 1989–2010.
9. Shepherd, A. G. A Mechanistic Analysis of Naphthenate and Carboxylate Soap-Forming Systems in Oilfield Exploration and Production. Heriot-Watt University, Edinburg, UK, 2008.
10. Qian, K.; Robbins, W. K.; Hughey, C. A.; Cooper, H. J.; Rodgers, R. P.; Marshall, A. G., Resolution and Identification of Elemental Compositions for More than 3000 Crude Acids in Heavy Petroleum by Negative-Ion Microelectrospray High-Field Fourier Transform Ion Cyclotron Resonance Mass Spectrometry. *Energy & Fuels* **2001,** 15, (6), 1505-1511.
11. Tomczyk, N. A.; Winans, R. E.; Shinn, J. H.; Robinson, R. C., On the Nature and Origin of Acidic Species in Petroleum. 1. Detailed Acid Type Distribution in a California Crude Oil. *Energy & Fuels* **2001,** 15, (6), 1498-1504.
12. Rudzinski, W. E.; Oehlers, L.; Zhang, Y.; Najera, B., Tandem Mass Spectrometric Characterization of Commercial Naphthenic Acids and a Maya Crude Oil. *Energy & Fuels* **2002,** 16, (5), 1178-1185.
13. Headley, J. V.; Peru, K. M.; Mohamed, M. H.; Frank, R. A.; Martin, J. W.; Hazewinkel, R. R. O.; Humphries, D.; Gurprasad, N. P.; Hewitt, L. M.; Muir, D. C. G.; Lindeman, D.; Strub,

R.; Young, R. F.; Grewer, D. M.; Whittal, R. M.; Fedorak, P. M.; Birkholz, D. A.; Hindle, R.; Reisdorph, R.; Wang, X.; Kasperski, K. L.; Hamilton, C.; Woudneh, M.; Wang, G.; Loescher, B.; Farwell, A.; Dixon, D. G.; Ross, M.; Pereira, A. D. S.; King, E.; Barrow, M. P.; Fahlman, B.; Bailey, J.; McMartin, D. W.; Borchers, C. H.; Ryan, C. H.; Toor, N. S.; Gillis, H. M.; Zuin, L.; Bickerton, G.; Mcmaster, M.; Sverko, E.; Shang, D.; Wilson, L. D.; Wrona, F. J., Chemical fingerprinting of naphthenic acids and oil sands process waters-A review of analytical methods for environmental samples. *Journal of Environmental Science and Health. Part A, Toxic/hazardous Substances & Environmental Engineering* **2013,** 48, 1145-1163.
14. Barrow, M. P.; McDonnell, L. A.; Feng, X.; Walker, J.; Derrick, P. J., Determination of the Nature of Naphthenic Acids Present in Crude Oils Using Nanospray Fourier Transform Ion Cyclotron Resonance Mass Spectrometry: The Continued Battle Against Corrosion. *Analytical Chemistry* **2003,** 75, (4), 860-866.
15. Ese, M.-H.; Kilpatrick, P. K., Stabilization of Water-in-Oil Emulsions by Naphthenic Acids and Their Salts: Model Compounds, Role of pH, and Soap : Acid Ratio. *Journal Of Dispersion Science And Technology* **2004,** 25, (3), 253-261.
16. Häger, M.; Ese, M. H.; Sjöblom, J., Emulsion Inversion in an Oil-Surfactant-Water System Based on Model Naphthenic Acids under Alkaline Conditions. *Journal of Dispersion Science and Technology* **2005,** 26, (6), 673-682.
17. Vindstad, J. E.; Bye, A. S.; Grande, K. V.; Hustad, B.; Hustvedt, E.; Nergård, B., Fighting Naphthenate Deposition at the Heidrun Field. In *International Symposium on Oilfield Scale*, Society of Petroleum Engineers: January 29-30th, Aberdeen, UK, SPE 80375, 2003.
18. Sarac, S.; Civan, F., Mechanisms, Parameters, and Modeling of Naphthenate-Soap-Induced Formation Damage. *Society of Petroleum Engineers Journal* **2009,** 14, (2), 259-266.
19. St. John, W. P.; Rughani, J.; Green, S. A.; McGinnis, G. D., Analysis and characterization of naphthenic acids by gas chromatography–electron impact mass spectrometry of tert.-butyldimethylsilyl derivatives. *Journal of Chromatography A* **1998,** 807, (2), 241-251.
20. Scott, A. C.; Young, R. F.; Fedorak, P. M., Comparison of GC–MS and FTIR methods for quantifying naphthenic acids in water samples. *Chemosphere* **2008,** 73, (8), 1258-1264.
21. Holowenko, F. M.; MacKinnon, M. D.; Fedorak, P. M., Characterization of naphthenic acids in oil sands wastewaters by gas chromatography-mass spectrometry. *Water Research* **2002,** 36, (11), 2843-2855.
22. Clemente, J. S.; Fedorak, P. M., A review of the occurrence, analyses, toxicity, and biodegradation of naphthenic acids. *Chemosphere* **2005,** 60, (5), 585-600.
23. Stanford, L. A.; Kim, S.; Klein, G. C.; Smith, D. F.; Rodgers, R. P.; Marshall, A. G., Identification of Water-Soluble Heavy Crude Oil Organic-Acids, Bases, and Neutrals by Electrospray Ionization and Field Desorption Ionization Fourier Transform Ion Cyclotron Resonance Mass Spectrometry. *Environmental Science & Technology* **2007,** 41, (8), 2696-2702.
24. Damasceno, F. C.; Gruber, L. D. A.; Geller, A. M.; Vaz de Campos, M. C.; Gomes, A. O.; Guimaraes, R. C. L.; Peres, V. F.; Jacques, R. A.; Caramao, E. B., Characterization of naphthenic acids using mass spectroscopy and chromatographic techniques: study of technical mixtures. *Analytical Methods* **2014,** 6, (3), 807-816.
25. Lewis, A. T.; Tekavec, T. N.; Jarvis, J. M.; Juyal, P.; McKenna, A. M.; Yen, A. T.; Rodgers, R. P., Evaluation of the Extraction Method and Characterization of Water-Soluble Organics from Produced Water by Fourier Transform Ion Cyclotron Resonance Mass Spectrometry. *Energy & Fuels* **2013,** 27, (4), 1846-1855.

26. Grewer, D. M.; Young, R. F.; Whittal, R. M.; Fedorak, P. M., Naphthenic acids and other acid-extractables in water samples from Alberta: what is being measured? *Science of the Total Environment* **2010,** 408, (23), 5997–6010.
27. Headley, J. V.; Peru, K. M.; McMartin, D. W.; Winkler, M., Determination of dissolved naphthenic acids in natural waters by using negative-ion electrospray mass spectrometry. *Journal of AOAC International* **2002,** 85, 182-187.
28. Clingenpeel, A. C.; Rowland, S. M.; Corilo, Y. E.; Zito, P.; Rodgers, R. P., Fractionation of Interfacial Material Reveals a Continuum of Acidic Species That Contribute to Stable Emulsion Formation. *Energy & Fuels* **2017,** 31, (6), 5933-5939.
29. Rowland, S. M.; Robbins, W. K.; Corilo, Y. E.; Marshall, A. G.; Rodgers, R. P., Solid-Phase Extraction Fractionation To Extend the Characterization of Naphthenic Acids in Crude Oil by Electrospray Ionization Fourier Transform Ion Cyclotron Resonance Mass Spectrometry. *Energy & Fuels* **2014,** 28, (8), 5043-5048.
30. Havre, T. E.; Sjöblom, J.; Vindstad, J. E., Oil/Water-Partitioning and Interfacial Behavior of Naphthenic Acids. *Journal of Dispersion Science and Technology* **2003,** 24, (6), 789-801.
31. Hurtevent, C.; Bourrel, M.; Rousseau, G.; Brocart, B., Production Issues of Acidic Petroleum Crude Oils. In *Emulsions and Emulsion Stability*, Sjöblom, J., Ed. CRC Press: Boca Raton, FL, USA, 2005; pp 477-516.
32. Celsie, A.; Parnis, J. M.; Mackay, D., Impact of temperature, pH, and salinity changes on the physico-chemical properties of model naphthenic acids. *Chemosphere* **2016,** 146, 40-50.
33. Bostick, D. T.; Luo, H.; Hindmarsh, B. *Characterization of soluble organics in produced water*; Oak Ridge, Tennessee, US, 2002; pp 25-26.
34. Havre, T. E. Formation of Calcium Naphthenate in Water/Oil Systems, Naphthenic Acid Chemistry and Emulsion Stability. PhD thesis, NTNU, Trondheim, Norway, Trondheim, 2002.
35. Brandal, Ø. Interfacial (o/w) Properties of Naphthenic Acids and Metal Naphthenates, Naphthenic Acid Characterization and Metal Naphthenate Inhibition. PhD thesis, NTNU, Trondheim, Norway, 2005.
36. Hanneseth, A. M. D.; Brandal, Ø.; Sjöblom, J., Formation, Growth, and Inhibition of Calcium Naphthenate Particles in Oil/Water Systems as Monitored by Means of Near Infrared Spectroscopy. *Journal of Dispersion Science and Technology* **2006,** 27, (2), 185-192.
37. Simon, S.; Reisen, C.; Bersås, A.; Sjöblom, J., Reaction Between Tetrameric Acids and Ca2+ in Oil/Water System. *Industrial & Engineering Chemistry Research* **2012,** 51, (16), 5669-5676.
38. Sjöblom, J.; Simon, S.; Xu, Z., The chemistry of tetrameric acids in petroleum. *Advances in Colloid and Interface Science* **2014,** 205, (0), 319-338.
39. Cooke, C. E., Jr.; Williams, R. E.; Kolodzie, P. A., Oil Recovery by Alkaline Waterflooding. *Journal of Petroleum Technology* **1974,** 26, (12), 1365-1374.
40. Speight, J. G., Chapter 4 - Effects in Refining. In *High Acid Crudes*, Speight, J. G., Ed. Gulf Professional Publishing: Boston, US, 2014; pp 77-109.
41. Dyer, S. J.; Graham, G. M.; Arnott, C., Naphthenate Scale Formation - Examination of Molecular Controls in Idealised Systems. In *International Symposium on Oilfield Scale, 29-30 January*, Society of Petroleum Engineers: Aberdeen, United Kingdom, 2003.
42. Mediaas, H.; Wolf, N. O.; Baugh, T. D.; Grande, K. V.; Vinstad, J. E., The Discovery of High Molecular Weight Naphthenic Acids (ARN Acid) Responsible for Calcium Naphthenate

Deposits. In *SPE International Symposium on Oilfield Scale, 11-12 May*, SPE 93011: Society of Petroleum Engineers: Aberdeen, United Kingdom, 2005.
43. Bertheussen, A.; Simon, S.; Sjöblom, J., Equilibrium partitioning of naphthenic acids and bases and their consequences on interfacial properties. *Colloids and Surfaces A: Physicochemical and Engineering Aspects* **2017,** 529, (Supplement C), 45-56.
44. Bertheussen, A.; Simon, S. C.; Sjoblom, J., Equilibrium partitioning of naphthenic acid mixture part 1: Commercial naphthenic acid mixture. *Energy & Fuels* **2018**.
45. Scherrer, R. A.; Howard, S. M., Use of distribution coefficients in quantitative structure-activity relationships. *J Med Chem* **1977,** 20, (1), 53-8.
46. Spildo, K.; Høiland, H., Interfacial Properties and Partitioning of 4-Heptylbenzoic Acid between Decane and Water. *Journal of Colloid and Interface Science* **1999,** 209, (1), 99-108.
47. Mediaas, H.; Grande, K. V.; Hustad, B. M.; Rasch, A.; Rueslåtten, H. G.; Vindstad, J. E., The Acid-IER Method - a Method for Selective Isolation of Carboxylic Acids from Crude Oils and Other Organic Solvents. In *International Symposium on Oilfield Scale, 29-30 January*, SPE 80404: Society of Petroleum Engineers: Aberdeen, United Kingdom, 2003.
48. Lide, D. R., CRC handbook of chemistry and physics: A ready-reference book of chemical and physical data. In 77 ed.; CRC Press Inc.: Boca Raton, Florida, US, 1997; p 842.
49. Lu, Y.; Wang, J.; Deng, Z.; Wu, H.; Deng, Q.; Tan, H.; Cao, L., Isolation and characterization of fatty acid methyl ester (FAME)-producing Streptomyces sp. S161 from sheep (Ovis aries) faeces. *Lett Appl Microbiol* **2013,** 57, (3), 200-5.
50. Barros, E. V.; Dias, H. P.; Pinto, F. E.; Gomes, A. O.; Moura, R. R.; Neto, A. C.; Freitas, J. C. C.; Aquije, G. M. F. V.; Vaz, B. G.; Romão, W., Characterization of Naphthenic Acids in Thermally Degraded Petroleum by ESI(−)-FT-ICR MS and 1H NMR after Solid-Phase Extraction and Liquid/Liquid Extraction. *Energy & Fuels* **2018,** 32, (3), 2878-2888.
51. Saab, J.; Mokbel, I.; Razzouk, A. C.; Ainous, N.; Zydowicz, N.; Jose, J., Quantitative Extraction Procedure of Naphthenic Acids Contained in Crude Oils. Characterization with Different Spectroscopic Methods. *Energy & Fuels* **2005,** 19, (2), 525-531.
52. Jones, D. M.; Watson, J. S.; Meredith, W.; Chen, M.; Bennett, B., Determination of Naphthenic Acids in Crude Oils Using Nonaqueous Ion Exchange Solid-Phase Extraction. *Analytical Chemistry* **2001,** 73, (3), 703-707.
53. Cassani, F.; Eglinton, G., Organic geochemistry of Venezuelan extra-heavy crude oils 2. Molecular assessment of biodegradation. *Chemical Geology* **1991,** 91, (4), 315-333.
54. Jones, D.; West, C. E.; Scarlett, A. G.; Frank, R. A.; Rowland, S. J., Isolation and estimation of the 'aromatic' naphthenic acid content of an oil sands process-affected water extract. *Journal of Chromatography A* **2012,** 1247, (1873-3778 (Electronic)), 171– 175.
55. Hemmingsen, P. V.; Kim, S.; Pettersen, H. E.; Rodgers, R. P.; Sjöblom, J.; Marshall, A. G., Structural Characterization and Interfacial Behavior of Acidic Compounds Extracted from a North Sea Oil. *Energy & Fuels* **2006,** 20, (5), 1980-1987.
56. ThermoScientific, Reagents, Solvents and Accessories catalogue. In 2012.
57. Acevedo, S.; Escobar, G.; Ranaudo, M. A.; Khazen, J.; Borges, B.; Pereira, J. C.; Méndez, B., Isolation and Characterization of Low and High Molecular Weight Acidic Compounds from Cerro Negro Extraheavy Crude Oil. Role of These Acids in the Interfacial Properties of the Crude Oil Emulsions. *Energy & Fuels* **1999,** 13, (2), 333-335.
58. Mapolelo, M. M.; Rodgers, R. P.; Blakney, G. T.; Yen, A. T.; Asomaning, S.; Marshall, A. G., Characterization of naphthenic acids in crude oils and naphthenates by electrospray

ionization FT-ICR mass spectrometry. *International Journal of Mass Spectrometry* **2011,** 300, (2–3), 149-157.
59. Wang, Z.; Hollebone, B. P.; Fingas, M.; Fieldhouse, B.; Sigouin, L.; Landriault, M.; Smith, P.; Noonan, J.; Thouin, G., Characteristics of Spilled Oils, Fuels, and Petroleum Products: 1. Composition and Properties of Selected Oils. In Research Triangle Park, North Carolina 27711, USA: Ecosystems Research Division, United States Environmental Protection Agency, 2003; p 286.
60. Seifert, W. K.; Teeter, R. M., Identification of polycyclic aromatic and heterocyclic crude oil carboxylic acids. *Analytical Chemistry* **1970,** 42, (7), 750-758.
61. Hindle, R.; Noestheden, M.; Peru, K.; Headley, J., Quantitative analysis of naphthenic acids in water by liquid chromatography–accurate mass time-of-flight mass spectrometry. *Journal of Chromatography A* **2013,** 1286, (Supplement C), 166-174.
62. Clemente, J. S.; Prasad, N. G. N.; MacKinnon, M. D.; Fedorak, P. M., A statistical comparison of naphthenic acids characterized by gas chromatography–mass spectrometry. *Chemosphere* **2003,** 50, (10), 1265-1274.
63. Brient, J. A.; Wessner, P. J.; Doyle, M. N., Naphthenic Acids. In *Encyclopedia of Chemical Technology*, Kirk-Othmer, Ed. John Wiley & Sons, Inc.: New York, 1995; pp 1017-1029.
64. Dewick, P. M., Acids and bases. In *Essentials of Organic Chemistry: For Students of Pharmacy, Medicinal Chemistry and Biological Chemistry*, Dewick, P. M., Ed. WILEY: West Sussex, England, 2006; p 130.
65. Passade-Boupat, N.; Rondon Gonzalez, M.; Hurtevent, C.; Brocart, B.; Palermo, T., Risk Assessment of Calcium Naphtenates and Separation Mechanisms of Acidic Crude Oil. In *SPE International Conference and Exhibition on Oilfield Scale*, Society of Petroleum Engineers: Aberdeen, UK, 30-31 May, SPE 155229, 2012.
66. Brown, A. M., A step-by-step guide to non-linear regression analysis of experimental data using a Microsoft Excel spreadsheet. *Comput Methods Programs Biomed* **2001,** 65, (3), 191-200.
67. Colin Cameron, A.; Windmeijer, F. A. G., An R-squared measure of goodness of fit for some common nonlinear regression models. *Journal of Econometrics* **1997,** 77, (2), 329-342.
68. Leo, A.; Hansch, C.; Elkins, D., Partition coefficients and their uses. *Chemical Reviews* **1971,** 71, (6), 525-616.
69. Leo, A. J., Calculating log Poct from structures. *Chemical Reviews* **1993,** 93, (4), 1281-1306.
70. Wang, R.; Fu, Y.; Lai, L., A New Atom-Additive Method for Calculating Partition Coefficients. *Journal of Chemical Information and Computer Sciences* **1997,** 37, (3), 615-621.
71. Cratin, P. D., Partitioning at the liquid-liquid interface. *Industrial & Engineering Chemistry* **1968,** 60, (9), 14-19.
72. Mukerjee, P., Dimerization of Anions of Long-Chain Fatty Acids in Aqueous Solutions and the Hydrophobic Properties of the Acids. *The Journal of Physical Chemistry* **1965,** 69, (9), 2821-2827.
73. Pestman, J. M.; Kevelam, J.; Blandamer, M. J.; van Doren, H. A.; Kellogg, R. M.; Engberts, J. B. F. N., Thermodynamics of Micellization of Nonionic Saccharide-Based N-Acyl-N-alkylaldosylamine and N-Acyl-N-alkylamino-1-deoxyalditol Surfactants. *Langmuir* **1999,** 15, (6), 2009-2014.

74. Heerklotz, H.; Epand, R. M., The Enthalpy of Acyl Chain Packing and the Apparent Water-Accessible Apolar Surface Area of Phospholipids. *Biophysical Journal* **2001,** 80, (1), 271-279.
75. Zhang, K.; Pereira, A. S.; Martin, J. W., Estimates of Octanol–Water Partitioning for Thousands of Dissolved Organic Species in Oil Sands Process-Affected Water. *Environmental Science & Technology* **2015,** 49, (14), 8907-8913.
76. Scarlett, A. G.; West, C. E.; Jones, D.; Galloway, T. S.; Rowland, S. J., Predicted toxicity of naphthenic acids present in oil sands process-affected waters to a range of environmental and human endpoints. *Sci Total Environ* **2012,** 425, 119-27.
77. Turner, A., Salting out of chemicals in estuaries: implications for contaminant partitioning and modelling. *Science of The Total Environment* **2003,** 314–316, 599-612.
78. Nordgård, E. L.; Ahmad, J.; Simon, S.; Sjöblom, J., Oil-Water Partitioning of a Synthetic Tetracarboxylic Acid as a Function of pH. *Journal of Dispersion Science and Technology* **2012,** 33, (6), 871-880.
79. Christiansen, I. Isolation and Characterization of Oil-Soluble Calcium Naphthenates in North Sea Heavy Crude Oil. M.Sc. Thesis, NTNU, Trondheim, Norway, 2014.